Universitetet i Stavanger

FACULTY OF SCIENCE AND TECHNOLOGY

MASTER'S THESIS

Study program/specialization: Petroleum Technology Reservoir Engineering	Spring semester, 2007 Open
Author: Martin Olsen	…… (signature author)

Instructor: Tor Austad

Supervisor: Skule Strand

Title of Master's Thesis:

Enhanced oil recovery in limestone. Chemical effects of seawater injection on the rock surface at different temperatures.

ECTS: 30

Subject headings: Limestone Wettability Potential determining ions	Pages: 70 + attachments/other: 15 Stavanger, 15th of June, 2007

Acknowledgement

I would like to thank Professor Tor Austad for giving me an interesting topic for my thesis, his excellent supervision and an opportunity to work for him.

I would like to thank Dr. Skule Strand for his excellent supervision, inspiring discussions and help at the laboratory.

I would like to thank Leif Ydstebø for his helping hand and guidance by using the Dionex ion chromatograph.

I would like to thank my colleague Sven Michael Feyling Barstad for the good teamwork during this thesis.

Finally I acknowledge the University of Stavanger and Petroleum engineering department for giving me good working conditions.

Department of Petroleum Technology, Stavanger, June 2007

Martin Olsen

Abstract

The fluid location, flow and distribution in a reservoir rock are to a large extent governed by the wetting condition of the rock. These factors influence oil and gas production, water flood recovery and the performance of enhanced oil recovery processes.

The wetting condition of carbonates is influenced by the surface chemistry of the rock. The impact of potential determining ions (Mg^{2+}, Ca^{2+} and SO_4^{2-}) on the rock surface at various temperatures (ambient, 80°C, 100°C and 130°C) on limestone cores from the Thamama field were carried out by slowly (1 PV/day) flooding the cores with synthetic seawater, SSW .

Chromatographic tests and spontaneous imbibition tests were also carried out. In the chromatographic tests different brine solution (SW-½M and SW-¼M) were flooded to detect the active surface area by the adsorption of SO_4^{2-}.

Spontaneous imbibition were carried out on several cores, both limestone and chalk, with increasing the temperature during the experimental time (ambient, 50°C and 70°C).

Both the spontaneous imbibition tests and chromatographic tests gave indication of the wettability.

From the experimental results obtained, major observations were:

- The cleaned limestone cores from the Thamama field behaved oil-wet during spontaneous imbibition tests.
- The water-wet surface area detected by the chromatographic test in the limestone cores was dependent on rate and concentration of SO_4^{2-}.
- Chromatographic test could be used on the limestone from Thamama field as identification on the wettability/fraction of water-wet surface area.
- The impact of potential determining ions in seawater was dependent on the temperature.

Table of content

1 Introduction

1.1 Carbonates

The carbonate rocks consist mainly of limestones and dolomites, these are composed largely of calcite, $CaCO_3$ and $CaMg(CO_3)_2$, respectively (Selly, 1998). Carbonate rocks are of varied origins. These origins are: detrital formed of debris, constructed of the reef type and chemical formed by the precipitation of bicarbonate, and originating in marine muds. Chalk and karst are two special cases of carbonate rocks. (Cossé, 1993). It is documented that close to 50% of the world proven petroleum reservoirs are located in carbonates, which usually show a rater low oil recovery factor, less then 30%, manly due to the wettability and the fractured nature of these reservoirs. The permeability of the matrix blocks is often in the range of 1-10 mD (Høgnesen et al, 2005. Manrique et al, 2006).

1.1.1 Limestone

Limestone is a sedimentary rock composed largely of the mineral calcite. Calcite is also called calcium carbonate; its chemical composition is $CaCO_3$. Limestone is found in many forms and is classified in terms of its origin, chemical composition, structure, and geological formation. (Siagi et al, 2007). Limestone and dolomites form some of the largest petroleum reservoirs in the world. Many of the biggest occur in the Middle East. Other areas in which carbonate reservoirs deliver large quantities of oil and gas are western Canada, Mexico, Texas (USA), Norway (central North Sea), Poland, Kazakhstan, western and southeastern China, Iran and Libya (Gluyas et al, 2004).

1.1.2 Chalk

Chalk is a special case of carbonates; it is formed by the stacking of small single-cell algae. This small single-cell algaes are called coccoliths (Cossé, 1993). Pelagic chalk diagenesis is the way the calcite skeletons of algal organisms, which provide the original material that becomes chalk, alter over geological time after settling on the ocean flow. The microstructure of the chalk is of great importance. The presence or absence of an organic coating on the chalk particles has consequences for wetting behavior (Andersen, 1995).The porosity of chalk is rather high, but the permeability in this carbonate is low or very low. It is about 1 mD. This

low permeability is by the pores been very small, in the range of 0.2 to 2 μm (Cossé, 1993). Chalk fields are generally of three types. Many are anticlines formed over salt domes. Others are formed by salt piercements. These forming mechanics give rise to fractures, some that are open and contribute to reservoir production and others that are not. (Andersen, 1995).

1.2 Enhanced oil recovery

Enhanced oil recovery, EOR, can be classified into three main steps:

- Primary recovery
- Secondary recovery
- Tertiary recovery

1.2.1 Primary Recovery

Primary recovery is the production of hydrocarbons from a reservoir by natural forces; no extra energy is used to produce the oil or gas. Only the pressure inside the reservoir will drive the hydrocarbons to the surface through the well. The pressure differences inside the reservoir will make the oil flow, from the high pressure zones to the lower pressure zones. This means, the oil will flow naturally from where the oil originally is trapped to the surface through the drilled well, only by the force of pressure differences.

1.2.2 Secondary Recovery

Secondary recovery is a physical method to enhance the oil production. It is also called, IOR, improved oil recovery. The secondary recovery technique often is used after the primary recovery method. After the primary production has been produced, the pressure inside the reservoir has decreased. Therefore, a pressure support is needed. This pressure support is established by injection a fluid into the reservoir. Water is the most common pressure supporter. The water will increase the pressure inside the reservoir around the injection well and force the remaining hydrocarbons to flow to the production well.

1.2.3 Tertiary recovery

When a reservoir has been exploited by both primary and secondary recovery techniques, there are still several percent left of the original hydrocarbons in place, OHIP. The remaining hydrocarbons can not be produced from the two mentioned techniques. The method for producing parts of the remaining hydrocarbons is called tertiary recovery. Tertiary recovery can be separated into four EOR processes.

- Mobility-Control Processes
- Chemical Processes
- Miscible Processes
- Thermal Processes

Mobility-Control Processes

This EOR process is using the injection fluid. The injection fluid is added polymers. By adding polymers, the viscosity of the fluid will increase and get a more favorable mobility ration when displacing the reservoir. The increase of viscosity will prevent fingering and increase the recovery.

Chemical Processes

By using chemical flooding as a tertiary recovery technique can be quite expensive. By adding surfactants into the injection fluid, the fluid will gain some advantageous properties. The interfacial tension between the fluids in the reservoir will decrease. This lowering of interfacial tension will make the fluids to mix, and can thereby be produced.

Miscible Processes

The primary objective in a miscible process is to displace hydrocarbons with a fluid that is miscible with the hydrocarbons. The two fluids will form a single phase mixed together. This single phase will make trapped oil producible.

Thermal Processes

Thermal processes are mainly based on the favorable properties of heated hydrocarbons. As the temperature inside the reservoir increases, the viscosity of the hydrocarbons decreases. The hydrocarbons will flow easier to the production well. Thermal processes can be

subdivided in to hot-water floods, steam processes, and in-situ combustion. (Green et al, 1998. Andersen, 1995).

1.3 Wettability in carbonates

Wettability as applied to an oil reservoir describes the tendency of a fluid to adhere or adsorb onto a solid surface in the presence of another immiscible fluid (Anderson, 1986). In contrast to sandstone reservoirs, literature data indicate that about 80-90% of the worlds carbonate reservoirs are preferentially oil-wet. (Høgnesen et al, 2005). Treiber et al measured the equilibrated water advancing contact angles of fifty crude oils. They found that of the carbonate reservoir-crude oil-water system tested, 8% were water-wet, 8% intermediate; and 84% oil-wet. This is in contrast to 43% water-wet; 7% intermediate; and 50% oil-wet for silicate formation reservoirs. (Hirasaki et al, 2003. Treiber et al, 1972). Studies by Austad el al (Austad et al, 2005. Zhang et al, 2005a. Tweheyo et al 2006) have show that secondary recovery, water injection, changes the wettability in chalk. The ions in the injected seawater chemically react with the solid surface and change the wettability index, in the more water-wet region. The seawater injection works as a chemical process in the tertiary recovery production.

2 Project Objectives

The objectives of this project are to identify and quantify the effects potential determining ions (Mg^{2+}, Ca^{2+} and SO_4^{2-}) in seawater mechanism toward limestone. Austad et al (2005) have studied the importance of the potential determining ions toward chalk. This study is of importance in oil recovery. 50% of the oil reserves in the world are in carbonates, most of them in limestone and dolomites (Høgnesen et al, 2005. Selly, 1998). The recoveries in these fields are relatively low, since most of them are in the oil-wet region. An improved understanding of the impact of potential determining ions in seawater on the wetting in limestone could have an influence on the recovery in limestone field across the world.

3 Theory

In this section the general principles and definitions of the fundamental concepts related to the main subjects of this thesis.

3.1 Displacement Forces

The flow of the different fluids inside a reservoir is influenced by several forces. In this chapter, the main three forces acting inside a core are described.

3.1.1 Gravity forces

The gravity force is very important in oil production, especially in oil/gas systems with the high difference between fluid phases. The gravity force is caused by the differences in density between two or more fluids. The fluid with the lowest density will have a tendency to flow upwards in the present of a more dense fluid. The gravity force can be expressed by formula 3.1 (Cole, 1969).

$$\Delta P_g = \Delta\rho \cdot g \cdot H \qquad 3.1$$

ΔP_g Pressure difference between oil and water due to gravity

$\Delta\rho$ Density difference between oil and water

g Acceleration due to gravity

H Height of liquid column

3.1.2 Viscous forces

Viscous forces in a porous medium are reflected in the magnitude of the pressure drop that occurs as a result of flow of a fluid through the medium. One approximation used to calculate the viscous force is to consider a porous medium as a bundle of parallel capillary tubes. With this assumption, the pressure drop for laminar flow through a single tube is given by Poiseuille's law given in equation 3.2.

$$\Delta p = -\frac{8\mu L\bar{v}}{r^2 g_c} \qquad 3.2$$

Δp pressure across the capillary tube

L capillary-tube length

r capillary-tube radius

$\overline{v}$ average velocity in the capillary tube

μ viscosity of flowing fluid

g_c conversion factor

3.1.3 Capillary forces

Petroleum reservoirs are complex systems. The petroleum reservoirs consists of water, oil, gas and the solid rock it self. In the reservoir there is a complex system where a mutual static interaction between the fluids and solid it self is formed.

Depending on the molecules in a particular fluid are attracted to each other by an electrical force or not, the fluid will be immiscible or miscible. These electrical forces are called cohesion. If the intra molecular fluid attraction is significantly larger than the inter fluid attraction, the two fluids will not mix, and the fluids behave immiscible. This is the general case for water, oil and gas. If the intra fluid molecular attraction is not significantly higher than the inter fluid attraction the fluid will mix. This is called the miscible state.

The electrostatic force will attract molecules in a fluid to the adjoining solid, this is called adhesion. If more than one fluid is present, the most adhesive fluid will be the wetting fluid (Zolotukhin et al, 2000).

*"Capillary pressure (P_c) can be defined as the molecular pressure difference across the interface of the two fluids" (*Zolotukhin et al, 2000, p.119*).*

The capillary forces are often the strongest force in multiphase flow. When there are more than one fluid present in a porous rock, there are at least three sets of active forces affecting the capillary force. These forces are active at the interface between the two immiscible fluid phases and between each fluid and the solid. The combination of all the active surface forces determines the capillary pressure of a porous rock (Skjæveland et al, 1992).

$$P_c = p_1 - p_2 \qquad 3.3$$

Formula 3.3 shows that the capillary pressure, P_c, is equal to the pressure difference, $p_1 - p_2$, across the interface of two fluids.

3.1.3.1 Capillary pressure in a tube

Figure 3.1 shows a simple drawing of two immiscible fluids inside a tube. The figure shows one wetting phase and one non-wetting phase. The interface between the two fluids will curve towards the wetting fluid.

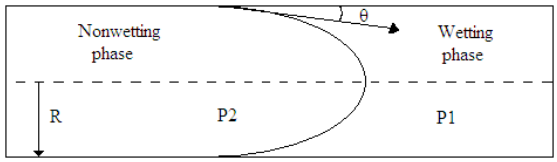

Figure 3.1. Two immiscible fluids inside a tube.

Formula 3.4 shows that the capillary pressure is dependent of several parameters. All these parameters are shown in figure 3.1. The capillary pressure is dependent of the pore structure of the porous rock, since *r* is the radius of the pore/tube. Both wettability and the interfacial tension influence the capillary pressure. Formula 3.4 shows that an increase in the interfacial tension between oil and water for this example, σ_{ow}, will give an increase in the capillary pressure. Wettability is also of great importance. The contact angle is the identification of wettability. This angle will decide whether the capillary pressure is a positive number or not. If the contact angle of the wetting fluid is larger than 90°, the capillary will become negative. When the angle is smaller than 90° the capillary pressure will be a positive pressure. In the extreme, if the contact angle is 90°, the capillary pressure will become zero. But this will not happen in the nature (Dake, 1978).

$$P_c = \frac{2\sigma_{ow}\cos\theta}{r} \qquad 3.4$$

P_c indicates the capillary pressure. σ_{ow} is the interfacial tension between the two immiscible fluids. θ indicates the contact angle, while *r* is the radii of the tube or pore.

3.1.3.2 Capillary Pressure across a Meniscal Interface

The interface of two immiscible fluids in a narrow cylindrical channel will normally be curved in the form of a menciscus. This curvature can be characterized by radius R_1 and R_2 shown in figure 3.2. Pressure differences between the two fluids will form this curvature. The interface will always be convex towards the wetting fluid.

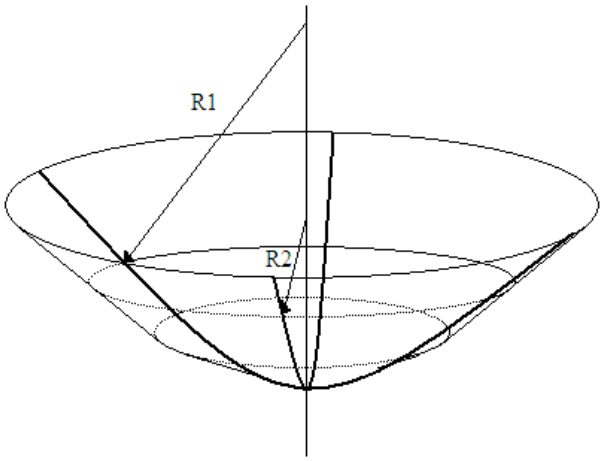

Figure 3.2. A meniscal interface

The wetting fluid will have a higher initial pressure. The relationship between the pressure difference and the curvature is shown in formula 3.5

$$\Delta p = P_c = \sigma\left(\frac{1}{R_1} + \frac{1}{R_2}\right) \qquad 3.5$$

R_1 and R_2 are the principal radii of the curvature and σ is the interfacial tension. If the meniscus is formed hemispherical, or a spherical oil droplet is equal in size as the pore size, R_1 and R_2 can be written as r and $\Delta p = 2\sigma/r$. For another extreme case, a planar interface both R_1 and R_2 will be equal to infinity, ∞, and Δp=0 (Zolotukhin et al, 2000).

3.1.4 Surface Tension and Interfacial tension

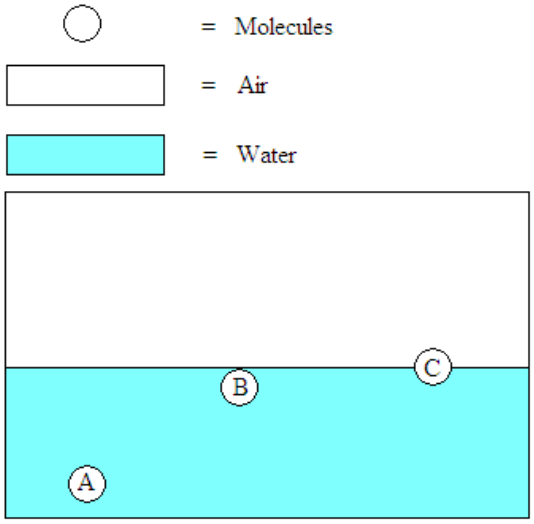

Figure 3.3. Free liquid surface indicating molecular positions.

In the contact between two fluids an interfacial tension, σ, will arise between them. The interface between to immiscible fluids can be considered as a membrane-like equilibrium surface. This membrane-like equilibrium surface is separating the phases with relative strong intermolecular cohesion and little or no molecular exchange (Zolotukhin et al, 2000).

When a liquid is not in contact with another liquid, but to air, the interfacial tension between the fluid and the air is called surface tension. A free liquid surface is illustrated in figure 3.3. In figure 3.3 A, B and C represent molecules of the liquid. At molecule A that is well below the surface the molecules are attracted equally in all directions owing to the cohesive forces. Because of this, the molecules movement tends to be unaffected by the cohesive forces. Molecule B and C, however, which are at or near the liquid/air interface, are acted on unequally. A net downward force tends to pull these molecules back into the bulk of the liquid. The surface thus acts like a stretched membrane, tending to shorten as much as possible. This surface force, which is a tensile force, is quantified in terms of surface tension (Green et al, 1998)

Depending on the relative magnitude of the intra- and inter fluid cohesive forces in fluids, the interfacial tension may have different signs. The signs can be separated into three main sign:

- $\sigma > 0$. When the interfacial tension is a positive number the molecules in the fluid are most strongly attracted to their own molecules. The fluid will be immiscible and not mix.

- $\sigma \approx 0$. When the interfacial tension is neutral molecules of each fluid are attracted equally to the other fluids molecules as they are attracted to their own molecules. The fluid will then become truly miscible.

– $\sigma < 0$. When the interfacial tension is a negative number the molecules in the fluid are more attracted to the molecules in the other fluid. The fluid will be miscible and mix.

Natural reservoir fluids will behave as immiscible fluids, although some gas may dissolve in the oil. Gases are generally miscible and show no interfacial tension, $\sigma \approx 0$ (Zolotukhin et al, 2000).

3.2 Wettability

Fluid distribution in porous media is not only affected by the forces at fluid/fluid interfaces, but also by the force at fluid/solid (Green et al, 1998).

"The wettability of a solid can be defined as the tendency of one fluid to spread on, or adhere to, the solid's surface in the presence of another immiscible fluid" (Zolotukhin et al, 2000, p. 116).

When two immiscible phases are placed in contact with a solid surface, one of the two fluids is usually attracted to the solids surface more strongly than the other fluid. The most strongly attracted phase is called the wetting phase.

Rock wettability is of great importance in oil production. The wettability affects both the nature of fluid saturations and it affects the general relative permeability characterizations of a fluid/rock system. Figure 3.4 shows the effect of saturations in a water-wet system and in an oil-wet system. The location of a phase within the pore structure determines the wettability of the system (Green et al, 1998).

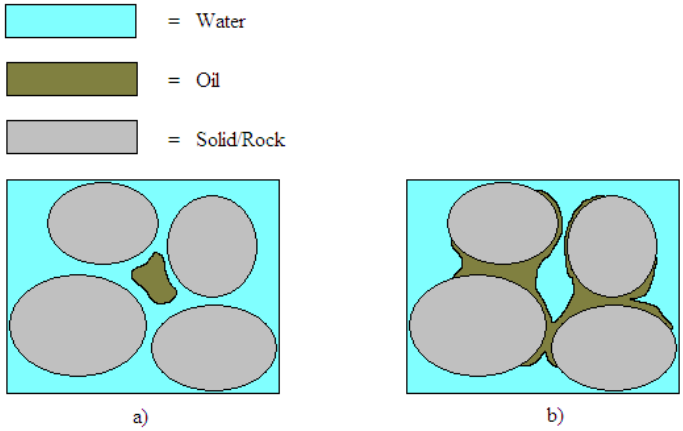

Figure 3.4. Effect of wettability on saturations.

In a rock/brine/oil system, water will displace oil if the surface is water-wet and vice versa if the surface is oil-wet. The wettability is of great importance when producing oil from subterranean formations. It is caused by all the important parameters for water and oil flow in a porous media. These parameters are: capillary pressure, relative permeabilities, fluid distribution, and flow directions (Strand et al, 2006). Considering the effect of wettability on fluid distributions, it is quite easy to rationalize that relative permeability curves are strong functions of wettability (Green et al, 1998).

The relative permeability is a strong function of the saturation phase, S, shown in figure 3.5. Being a rock-fluid property, the function between relative permeability and saturation is a function of rock properties (e.g. pore size distribution) and wettability.

Rocks are also known to have intermediate and/or mixed wettability. It is depending on the physical/chemical makeup of the rock. The wettability is also depending on the composition of the oil phase. Intermediate wettability occurs when both phases tend to adsorb to the rock surface, but one phase will always be slightly more attracted to the surface than the other. Mixed wettability is a result of variation or heterogeneities in chemical composition of the exposed rock surface or cementing-material surface in the pores. Wettability conditions may vary from point to point because of this mixed chemical exposure. Water sometimes wets the solid over part of the surface and oil over the remaining part of the surface (Green et al, 1998. Dake, 1994).

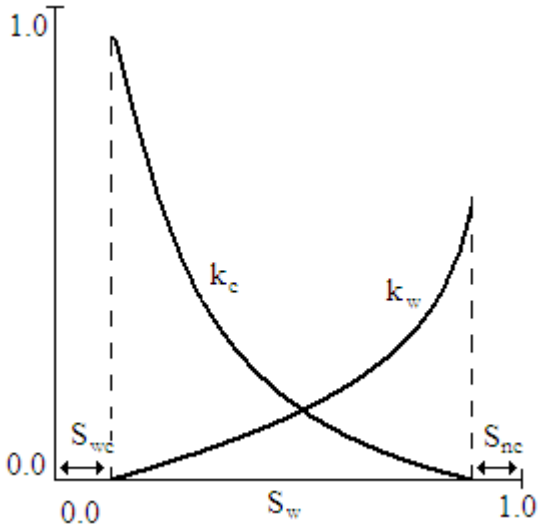

Figure 3.5. Typical type of relative permeability characteristics for a two phase flow.

3.2.1 Wetting state of a reservoir

The wetting state of a reservoir is the result of absorption of polar components from the crude oil onto the originally strongly water-wet mineral surface. Clean carbonate rocks are naturally water-wet. Most of the oil producing reservoirs were originally water-wet before the oil migrated from the source rock into the reservoir formation. When oil first invades a pore, the solid surface is coated by a thick wetting film of water. When a critical capillary pressure is exceeded, the water film rupture, resulting in direct contact of crude oil with the pore wall. Surface-active components of the crude deposit on the rock surface, rendering it oil-wet. This absorption of polar components from the crude oil will most likely take place where the rocks surface is directly exposed to the oil-phase (Al-Hadhrami et al, 2001. Strand et al, 2006).

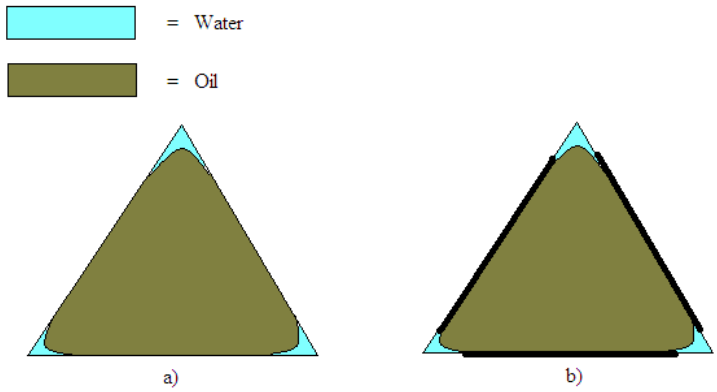

Figure 3.6. Oil and water in triangular pore.

Figure 3.6 illustrates this process. Oil and water is in a triangular pore. When oil enters a pore during primary oil migration, the pore is water wet. Figure 3.6.a illustrates the water-wet system. However, surface active components in the crude oil may adhere to the portions of the solid surface directly in contact with the oil. The change in wettability is shown in figure 3.6.b. The thick bold lines indicate regions of the surface that are oil-wet. By heating, this process can be reversed on calcite surfaces. The surface active components desorbs, leaving a water-wet surface (Al-Hadhrami et al, 2001).

3.2.2 Calcite surface

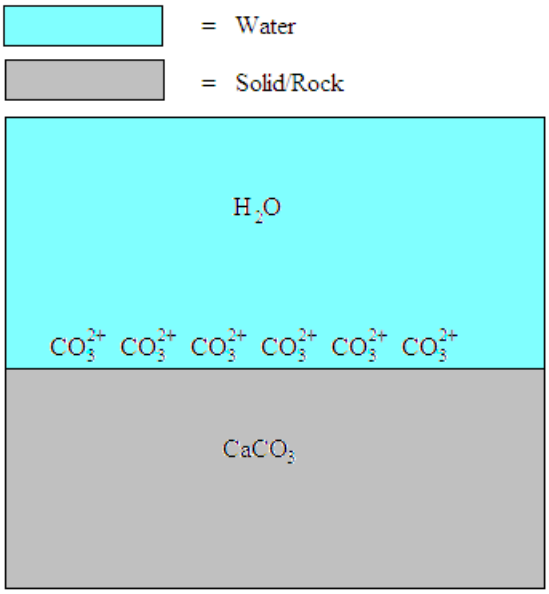

Figure 3.7. Calcite surface

The type of mineral surface in a reservoir is important in determining the wettability. Carbonate reservoirs are typically more oil-wet than sandstone reservoirs. The carbonates are composed largely of calcite ($CaCO_3$). Carbonates tend to adsorb simple organic acids. This occurs since carbonates have a positively charged, weakly basic surface. This is illustrated in figure 3.7. Reaction 3.1 shows the reaction on the carbonates surface which makes is weakly basic (Anderson, 1986).

$$CO_3^{2+} + H_2O \rightarrow HCO_3^- + OH^- \qquad 3.1$$

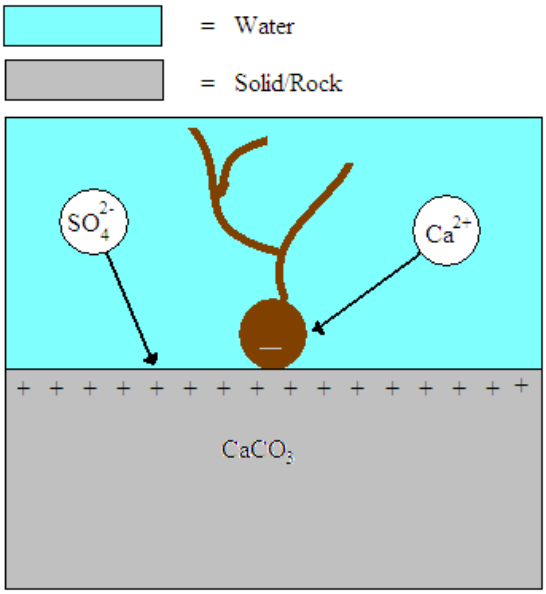

Figure 3.8. Wettability alteration mechanism in chalk.

The calcite surface will preferentially adsorb components of the opposite polarity, in this case acidity, by an acid/base reaction (Anderson, 1986). This acid-base interaction between the solid and oil is a strong polar interaction. It is hard to separate the oil and solid. Studies by Strand et al (2005) have suggested a wettability alternation in chalk. This is illustrated in figure 3.8. The desorption of carboxylic materials from the surface involving both a change in the surface charge by adsorption of SO_4^{2-} and the contribution from Ca^{2+} to release the carboxylic group. These two ions are in the composition of seawater. The sulfate ion adsorbs to the positively charged surface, this gives room for the calcium ions to interact with the acidly organics on break the strong acid-base interaction and free the oil from the chalk surface and make the solid more water-wet.

3.3 Wettability measurements

The wettability can be measured by several different methods. In this section some of these methods are described.

3.3.1 Contact Angle

The wettability of a rock can be quantified by the contact angel between the wetting fluid and the solid or another fluid and the interfacial tension. It can be quantified by formula 3.6. Formula 3.6 is a force balance at the line of intersection of solid, water and oil.

$$\sigma_{os} - \sigma_{ws} = \sigma_{ow} \cos\theta \qquad 3.6$$

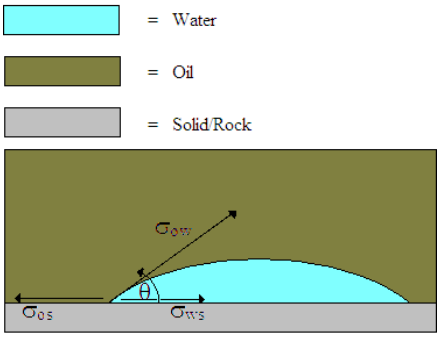

Figure 3.9. Interfacial forces at an interface between two immiscible fluids and a solid.

σ_{os} is the interfacial tension, IFT, between the oil and the solid. σ_{ws} indicates the IFT between the water and the solid and likewise with σ_{ow}, indicating IFT between oil and water. θ is the contact angle measured through the water. σ_{os}, σ_{ws}, σ_{ow} and θ are also shown in figure 3.9.

The interfacial tension between oil σ_{ow}, and water can easily be determined by using a ring tensiometer or for ultra low IFT a spinning drop tensiometer can be used. The interfacial tension between water and solid, σ_{ws}, and the interfacial tension between oil and the solid rock, σ_{os}, can not be measured. Experimental have not been developed to measure these two interfacial tensions. Therefore, the contact angle has to be measured to determine/calculate the wettability (Green et al, 1998). This angle can be measured with a camera, but only on crystal surfaces. A picture is taken of the liquid adsorbed to the solid surface and measured.

Figure 3.10 shows changes in contact angle. The contact angle may vary from 0° to 180°; from 100% water wet system, figure 3.10.a, to 100% oil-wet system. As mentioned the contact angle determines the wettability. The wettability be classified depending of the degrees of the contact angle. Table 3.1 shows contact angle versus wettability preference

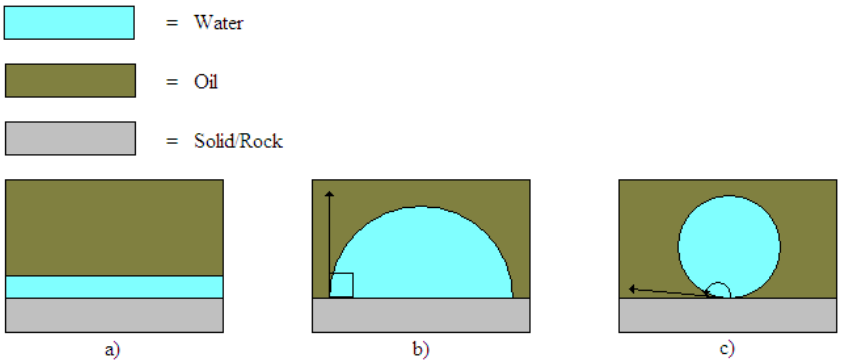

Figure 3.10. Hypothetical end-member cases of the wetting preference of different solids by a water and oil system

Table 3.1. Wetting angle vs. wettability preference.

Wetting angle	Wettability preference
0°-30°	Strongly water-wet
30°-90°	Preferentially water-wet
90°	Neutral wettability
90°-150°	Preferentially oil-wet
150°-180°	Strongly

According to William G. Anderson (1986) the contact angle is temperature dependent. Measurements through the water, shown in figure 3.9 and 3.10, have shown that the contact angle will decrease as the temperature is increased. The decrease in contact angle will make the system become more water-wet (Al-Hadhrami et al, 2001).

3.3.2 Amott indices

Wettability can also be determined from displacement experiments. This method is considered to be indirect method, since it requires saturation measurements during the oil and brine displacement or capillary pressure data. In the Amott test, water is first displaced by oil by centrifugal or by use of a high flowing pressure gradient. Pressure levels and time taken to reach initial water saturation, S_{wi} , are somewhat arbitrary. The aim should be to begin at the same water saturation as in the reservoir. The core at initial water saturation is then immersed

in water to allow spontaneous imbibition. Spontaneous imbibition of water ceases at some change in water saturation, ΔS_{ws}, when oil/water surface curvature falls to zero. Further oil can usually be recovered by forced displacement to give an overall increase in water saturation, ΔS_{wt}, by flooding water at a high pressure gradient or centrifuging. From figure 3.11 the Amott indices can be determined be using capillary pressure curve.

$$I_w = \frac{\Delta S_{ws}}{1 - S_{wi} - S_{or}} = \frac{\Delta S_{ws}}{\Delta S_{wt}} \qquad 3.7$$

$$I_o = \frac{\Delta S_{os}}{1 - S_{wi} - S_{or}} = \frac{\Delta S_{os}}{\Delta S_{ot}} \qquad 3.8$$

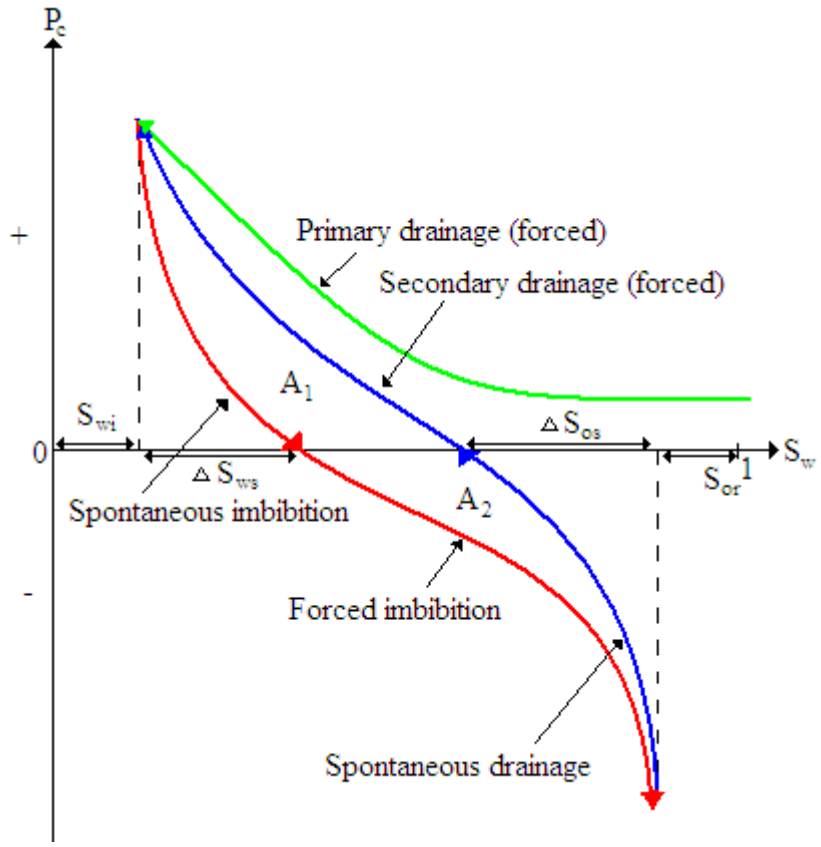

Figure 3.11. Capillary pressure diagram used to characterize wettability.

ΔS_{ws} Increase in water saturation during spontaneous imbibition of water.

ΔS_{os} Increase in oil saturation during spontaneous imbibition of oil.

ΔS_{wt} Total increase in water saturation during spontaneous and forced displacement of oil.

ΔS_{ot} Total increase in oil saturation during spontaneous and forced imbibition of water.

S_{or} Residual oil saturation

S_{wi} Initial water saturation

Completely water-wet gives $I_w = 1$ and $I_o = 0$, while completely oil-wet gives $I_o = 1$ and $I_w = 0$.

Amott-Harvey index can also be calculated be the same saturations as described above. Amott-Harvey index may be calculated directly form formula 3.9

$$IAH = I_w - I_o = \frac{\Delta S_{ws} - \Delta S_{os}}{1 - S_{wi} - S_{or}} \qquad 3.9$$

The Amott-Harvey index ranges from 1 for a completely water-wet system to -1 for a completely oil-wet system (Morrow, 1990. Strand et al, 2006)

3.3.3 USBM method

In the USBM method drainage and imbibition capillary pressures are measured, most commonly by centrifuge. As with the Amott test, the method was developed from observation of crude-oil/brine/rock displacement behavior. The wettability number is defined by formula 3.10 (Morrow, 1990).

$$N_w = \log \frac{A_1}{A_2} \qquad 3.10$$

A_1 Area under the secondary water-drainage curve, shown in figure 3.11.

A_2 Area under the imbibition curve falling bellow the zero-P_c axis, shown in figure 3.11.

The advantages of this method are the speed and simplicity of the procedure and its adaptation to the relative permeability measurements. But there are some correlations that most be applied to the average saturations measured by centrifuge. The claimed thermodynamics basis

for the method that equates work of displacement to change in surface free energy does nor recognize the effects of irreversibility in capillary pressure relationships, and systems that imbibe to give positive A_2, for example very strongly water-wet systems, are not recognized in the proposed interpretation.

3.3.4 Imbibition rates

The driving force for spontaneous imbibition rates is the capillary pressure. Spontaneous imbibition measurements provide a useful support to the two Amott indices or USBM wettability number (Morrow, 1990). The main difference between the Amott test and the imbibition rates are what they are dependent of. Amott test depends mainly on the saturation at which imbibition capillary pressure falls to zero. Spontaneous imbibition rate depends on the magnitude of the imbibition capillary pressure. Measurements of imbibition rates are of special value as a sensitive measure of wetting in the range where Amott index is or close to unity. Measurements of imbibition rates also provide information on dynamic IFT and wetting phenomena that may be important in the reservoir but are not reflected by Amott or USBM wettability test

3.3.5 New wettability test for carbonates

Strand et al (2006) have come up with a new method to determine the wettability index of chalk. The wettability test is based on the chromatographic separation of two water-soluble components, i.e. a tracer, SCN^-, and a potential determining ion towards chalk, SO_4^{2-}. Chromatographic separation will only take place at the water-wet sites at the pore surface. The fraction of the surface area covered by water was decided to represent the new wetting index.

Strand et al (2006) studies and experiments were performed on chalk cores. Chalk cores with residual oil were used. It was shown that the area between the effluent curves for SCN^- and SO_4^{2-} was proportional to the area contacted by water during flooding process. The ratio between this area and the corresponding area obtained from a completely water-wet core will give a water index between 0 and 1, representing completely oil-wet and completely water-wet conditions, respectively. The method was proven to be an excellent wettability test close to neutral conditions; witch will give a wetting index of 0.5.

First a S_{or} should be established. Core most be aged in oil and then shaved, to prevent skin. The saturation can be established by flooding the core with on pore volume with brine without tracer and sulfate at a defined rate, followed by 1 pore volume of the same brine with a doubling of the rate. Total displaced oil volume can be measured, and the S_{or} –value can be calculated.

According to Strand et al (2006) the core should be flooded with at least 2 pore volumes with brine containing sulfate or tracer. Small fractions of the effluent have to be collected. The exact volume and pore volume of each fraction could then be calculated using the weight and the density of the fluid. Each fraction has to be analyzed for the relative concentrations of sulfate and thiocyanate, and be plotted against pore volume injected. The delay in the sulfate concentration compared to the thiocyanate concentration in the effluent is proportional to the pore surface accessible to adsorption. When S_{or} –value has been calculated and the fractions of the effluent have been collected and analyzed the wettability index can be calculated from formula 3.11

$$WI_{New} = \frac{A_{Wett}}{A_{Hep\tan e}} \qquad 3.11$$

A_{Wett} Area between the thiocyanate and the sulfate curves generated by flooding a core aged in crude oil.

$A_{Heptane}$ Reference area between the thiocyanate and sulfate curves generated by flooding a core assumed to be strongly water-wet (saturated with heptane)

The area between the two curves can be calculated by subtraction of the area under each of the curves by the trapeze method (Strand et al, 2006).

4 Experimental work

4.1 Pre-experiments

4.1.1 Core determination

Before the main experiments of this thesis could start, cores had to be selected. To decide witch core had the most advantageous potential, a spontaneous imbibition test was carried out on three cores. Two potential experimental limestone cores was picked and one chalk core. Core number 12D and 20A were the chosen limestone cores. The limestone cores used were from a reservoir filed in the Middle East, and had different permeabilities and pore structure. The chalk core used was outcrop chalk from Stevens Klint. Figure 4.1 shows a chalk core and a limestone core. The limestone core 20A was chosen because it had approximated the same permeability as the chalk core. All limestone cores had been used in previous experiments, thereby the permeability and porosity was known. The cores that had been used in previous experiments had all been washed by the same washing method. This washing method is described later in this chapter 4.1.4.

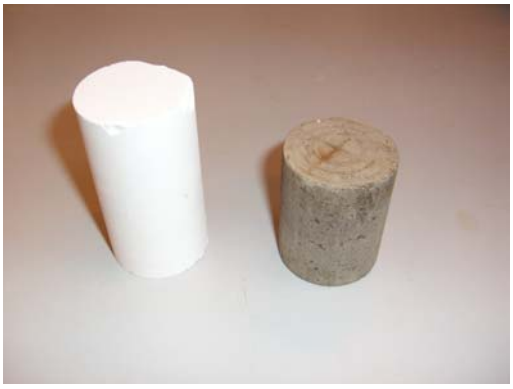

Figure 4.1. Chalk core and limestone core

Thamama field

The limestone cores used in the experiments are from the Thamama field. The Thamama field is located onshore in the Middle East. The Thamama formation is a low permeable formation, ranging form 0.3 mD to just above 70 mD. The reservoir is a layer cake type reservoir. This layer cake type reservoir has wide stratas that are only a few feet high. The overall permeability increases upwards. The formation may be divided into two zones, the Upper zone and the Lower zone. The Lower layer consists of only low permeable layer, while the Upper layer is composed of high permeable porous limestone layers separated by low permeable stylolitic layers (Namba et al, 1995).

Stevns Klint

The chalk core used in the experiment is from an outcrop from Stevns Klint nearby Copenhagen, Denmark. The Stevns Klint chalk is a soft and highly porous material of Maastrichian age. The chalk is mainly composed of fine-graded coccolithic matrix. The porosity is high, in the range of 45% to 50%. The permeability is relatively low, in the range of 1 mD to 3 mD (Strand et al, 2006).

4.1.2 Saturation of cores

To perform the spontaneous imbibition tests, the cores had to be saturated with oil. The three cores were saturated with heptane. The reason that heptane was used, was the advantageous density of the heptane and it probably would imbibe relatively fast. The cores were placed and evacuated in a container as shown in figure 4.2. When a satisfying vacuum pressure had been reached, heptane was slowly injected into the bowl. The cores stayed in heptane over the night to obtain 100% heptane saturation. Before the cores got saturated with heptane; weight, length and diameter were measured. After the saturation process the cores were weight again. From these measurements the pore volume and porosity could be calculated from formula 4.1 and 4.2.

Figure 4.2. Saturation container

$$V_p = \frac{W_{wet} - W_{dry}}{\rho_{fluid}} \qquad 4.1$$

V_p indicates the pore volume. W_{wet} is weight of the core when saturated, while W_{dry} is the weight of the core before saturation. ρ is the density of saturation fluid.

$$\phi = \frac{V_p}{V_b} \qquad 4.2$$

ϕ indicates the porosity. This number can be multiplied by 100 to get the porosity in percent. V_p is the pore volume and V_b is the bulk volume.

Table 4.1 shows the result of the calculation of porosity and pore volume for the cores used in the spontaneous imbibition experiments.

Table 4.1. Core data of cores used in imbibition experiments

Core #	Type	Ø [cm]	L [cm]	V [cm3]	ϕ [%]	k [mD]	m_0 [g]	m [g]	Weight heptane [g]	IOIP [ml]
12D	Lime-stone	3,780	4,810	53,95	26,89	20,40	105,42	115,33	9,91	14,51
20A	Lime-stone	3,790	4,890	55,14	26,26	3,03	108,98	118,87	9,89	14,48
SK	Chalk	3,750	5,260	58,07	47,93	-	80,82	99,83	19,01	27,83

4.1.3 Spontaneous Imbibition

The three 100% heptane saturated cores were placed in Amott cells. An imbibition cell is shown in figure 4.3. 12D, 20A and SK were the cores used in the spontaneous imbibition experiments. SK was known to be water-wet. 12D and 20A were the limestone cores. The cores were placed inside of the imbibition cells to see if they would spontaneous imbibe. If they imbibed, this could be an indication of a water-wet system.

Figure 4.3. Amott cell

The chalk core, SK, was imbibed simultaneously. Synthetic seawater, SSW, was chosen as imbibition brine. The composition of this SSW brine is listed in table 4.2. Limestone core 12D and

20A were chosen; because of the permeability difference between these two cores. 20A has a low permeability like the chalk, and 12D a relatively high. Since spontaneous imbibition is dependent of the capillary pressure, the core with the lowest permeability was assumed to be core that would imbibe the most quickly. Since the capillary pressure is dependent of the pore radius, formula 3.3, it was assumed that the core with the lowest permeability also has got the smallest pore radius. The core that would gain the highest oil recovery would be assumed to be the most water-wet core. The results will be discussed later in chapter 5.1

4.1.4 Core Cleaning

As mentioned the limestone cores had been used in the earlier experiments and needed to be washed. All cores were cleaned by the same washing method. This was conducted to remove the remaining oil and to give the cores the same wetting properties, as water-wet as possible.

The cleaning process was accomplished by flooding every core with toluene and methanol at ambient temperature. These two liquids cleaned the core inside, and forced oil and other materials from previous experiments out of the core. First 5 PV of toluene was until clean toluene was observed at the outlet, and then 5 PV methanol was flooded through the cores. Finally 5 PV with distilled water was flooded, before the cores were placed in a heat chamber to evaporate remaining fluids.

4.1.5 Brines

In the experimental work, several brines have been used. The composition of these brines is listed in table 4.2. The brines were prepared in the laboratory from distilled water and salt.

Table 4.2. Brine formulation

Salt	SSW		SW-U		SW-½M		SW-¼M	
	[g/l]	[mole/l]	[g/l]	[mole/l]	[g/l]	[mole/l]	[g/l]	[mole/l]
NaCl	23,38	0,400	29,12	0,498	26,25	0,449	27,10	0,464
Na_2SO_4	3,41	0,024	-	-	1,71	0,012	0,85	0,006
KSCN	-	-	-	-	1,17	0,012	1,17	0,012
$NaHCO_3$	0,17	0,002	0,17	0,002	0,17	0,002	0,17	0,002
KCl	0,75	0,010	0,75	0,010	0,75	0,010	0,75	0,010
$MgCl_2 \times 6H_2O$	9,05	0,045	9,05	0,045	9,05	0,045	9,05	0,045
$CaCl_2 \times 2H_2O$	1,91	0,013	1,91	0,013	1,91	0,013	1,91	0,013

The SSW brine is synthetic seawater. SW-U is a modification of SSW. This brine is without sulfate and thiocyanate. The brine SW-½M is modified seawater with half the sulfate concentration and thiocyanate as tracer. SW-¼M is modified seawater with forth the sulfate concentration.

SSW was used in the spontaneous imbibition experiments and the adsorption experiments. SW-U, SW-½M and SW-¼M were used in chromatographic studies.

4.2 Chromatographic studies of active surface area

To determine the active surface area inside the limestone cores, the same principal setup as used by Strand et al (2006) to determine the new wettability index. This method is mentioned in chapter 3.3.5. The active surface area, A_{Wett}, was calculated. The wettability index, formula 3.11, it self is not calculated in this thesis since $A_{Heptane}$ was unknown.

4.2.1 Flooding composition

A Hassler cell was used to flood the core. As shown in figure 4.4. The core was placed inside a core sleeve. The core and core sleeve were placed inside the Hassler cell. Outlet and inlet were attached to the sides of the Hassler cell, so the brine would flow through it. The Hassler cell was screwed together to obtain the pressure that would occur inside the cell when the experiments started. Around the core a confining pressure was established. This pressure was about 20 bars by using nitrogen. The objective of the confining pressure was to compress the core sleeve around the core. This was of great importance, so the brine would flow through the core, and not take the easiest way around it.

Figure 4.4. Hassler cell

As a driving force for flowing of the core, a Gilson 307 HPCL piston pump was used, shown in figure 4.5. The HPCL pump pumped distilled water form a water reservoir into two piston cells. One of the piston cells containing SW-U and the other cell containing SW-½M or SW-¼M. Both SW-½M and SW-¼M were used in this flowing composition, but not at the same time. SW-U was used through out the entire experiment. Not more than one fluid was flowing through the core at once. To control the brine flow a valve on top of piston cell was used. The valve made it easy to change the flow of one brine to another brine. The brine was flowing directly from the piston cell to the Hassler cell containing the core.

Figure 4.5. Gilson 307 HPCL piston pump

On the outlet of the Hassler cell a valve system was attached. With these valves the outlet flow could be controlled. The flow could be steered into a waist container or a fraction collector (Gilson 222 XL Liquid Handler). The collector could be programmed to collect a specified amount of effluent in small glass jars. These samples was then diluted with distilled water and analyzed.

4.2.2 Rate optimization

Before the main chromatographic studies could be carried out, an optimum injection rate had to be decided. The rate with the most piston-like displacement of the core would be the optimal rate for the pump.

Earlier studies preformed on chalk have shown that the rate should be in the range of 0.1ml/min and 0.2 ml/min (Strand et al, 2006). A cleaned (chapter 4.1.4) limestone core, number 2-21, was used. It was saturated by the same method as mentioned in chapter 4.2.1, except this time with SW-U instead of heptane. This core had also been used in previous experiment. Core 2-21 was placed inside the Hassler cell as explained earlier. The brines used in this optimization were SW-U and SW-½M (table 4.2).

First a couple pore volumes of SW-U was flooded through the core with a relatively high rate. This was done to get the core completely saturated with SW-U even though it was saturated with SW-U, then the core was flooded with one pore volume SW-U at the same rate as used in the optimization. The reason for this was to ensure chemical and pressure equilibrium inside the core. After equilibrium was reached, SW-½M brine was flooded through the core. A rate of 0.2 ml/min was used.

The effluent from the core was collected in small glasses with the collector. The collector was programmed to take samples at a defined time space. Every sample was weight. Since the glasses were weight in advance the precise amount of effluent could be measured. By simple subtraction the exact pore volume was calculated. The samples were analyzed chemically to detect the concentration of both thiocyanate and sulfate. The chemical analyzing methods are mention in chapter 4.2.3. The relative concentration C/C_0 of the two anions was plotted against the PV injected. C_0 is concentration of anions in the initial fluid (SW-½M). The relative concentration of the tracer thiocyanate will detect the injection front. The area of delay between the thiocyanate curve and sulfate curve would indicate whether or not there was an active surface area (Strand et al 2006).

A new test was carried out on the same core using the same procedure with a rate of 0.1 ml/min. The core data of core number 2-21 is listed in table 4.3 together with the other cores used for adsorption testing and chromatographic studies. The results are discussed in chapter 5.2.1.

Table 4.3 Core data of cores used in the main experiment

Core #	Type	Ø [cm]	L [cm]	V [cm3]	ϕ [%]	k [mD]	m_0 [g]	m [g]	Weight brine [g]	IOIP [ml]
2-21	Lime-stone	3,795	4,920	55,62	24,40	2,70	112,88	126,78	13,90	13,57
20A	Lime-stone	3,790	4,895	55,20	25,60	3,03	108,95	123,42	14,47	14,13
46A	Lime-stone	3,795	4,775	53,98	26,95	2,47	104,65	119,55	14,90	14,55

4.2.3 Chemical analysis

The sampled effluents from the core flooding tests were analyzed in order to detect changes in initial fluid composition. In the experimental work in this thesis two different types of chemical analysis were used. Spectroquant photometer NOVA 60 and ion chromatograph were used. Spectroquant photometer NOVA 60 was used for rate optimalizaton and the ion chromatograph was used in the other experiments.

Spectroquant photometer NOVA 60

Figure 4.6. Spectroquant photometer NOVA 60

Brine samples were analyzed with a Spectroquant photometer NOVA 60. This instrument was able to measure both the concentration of thiocyanate and sulfate. Spectroquant photometer NOVA 60 is shown in figure 4.6.

Sulfate, SO_4^{2-}

The SO_4^{2-} concentration could be determined. The fraction of the effluent had to be diluted to get into the measuring range concentration of the instrument. The instrument could measure in the range of 5-250 mg/l. The initial concentration of sulfate in SW-½M is 1150 mg/l. The fractions of the effluent were diluted with distilled water in 1:10 proportion. To the diluted fractions the reaction ion barium, Ba^{2+}, was added. The reaction between sulfate and barium created barium sulfate, $BaSO_4$. This is shown in reaction 4.1.

$$Ba^{2+} + SO_4^{2-} \rightarrow BaSO_4 \qquad 4.1$$

The $BaSO_4$ creates a blackening of the effluent. The Spectroquant photometer NOVA 60 measured the degree of blackening. From this degree of blackening a concentration of sulfate was given.

Thiocyanate SCN^-

The thiocyanate concentration was analyzed by diluting an exact sample volume with 0.2 M solution of $Fe(NO_3)_3$ dissolved in 1.0 M HNO_3 solution. When the concentration of Fe^{3+} was

significantly higher than the thiocyanate concentration, all thiocyanate ions would be converted to the thiocyanate complex ion $FeSCN^{2+}$. This is shown in reaction 4.2.

$$Fe^{3+} + SCN^{-} \rightarrow FeSCN^{2+} \qquad 4.2$$

The $FeSCN^{2+}$ solution has got a deep red color. The absorbance was measured with the Spectroquant photometer NOVA 60 at 445nm. From the degree of absorbance a concentration of thiocyanate was given. This concentration divided by the concentration of thiocyanate in the original brine gave the relative concentration.

Ion chromatography

An ion chromatograph measures the concentration of inions in a solvent with very high accuracy. Ion exchange chromatography is a process that allows the separation of ions and polar molecules based on the charge properties of the molecules. The ion chromatograph used in the experiments was delivered by Dionex. It was constructed to measure concentrations of both anions and cations simultaneously. The ion chromatograph is shown in figure 4.7.

Figure 4.7. Dionex ion chromatograph

Before the solvent could be analyzed by the ion chromatograph the effluent had to be diluted. Two standard solvents had to be made. The standard solvents were the initial fluid diluted in 1:20 and 1:100 when SW-½M and SSW were used. When SW-¼M was used as the standard solvent it was diluted into two standards at 1:10 and 1:50. These standards were used to find the relative concentrations, C/C_0. The reason for diluting the standards into two difference concentrations was to construct a calibration curve. A new calibration curve was constructed automatically each time the ion chromatograph was used.

After the standards were diluted into two concentrations, the samples also had to be diluted. The samples were always diluted in at the same range as the standard with highest concentration. Meaning that with SW-½M and SSW as standards, the samples were diluted at 1:20. The SW-¼M standards were diluted into 1:10.

After the samples were diluted they had to be filtrated. The filtration was easily accomplished with a syringe filter. The samples had to be filtered to prevent particles to enter the columns inside the ion chromatograph, since these were very sensitive to particles. Particles may easily block the tubing and cause an over pressure.

4.3 Chromatographic studies with variations in sulfate concentration.

When an optimum rate was decided, the chromatographic studies with variations of sulfate concentration in the brine could be carried out. In the chromatographic experiments the same setup for rate optimization was used. The same limestone core, 2-21, was used. It was placed inside the Hassler core and flooded with brine solutions as described in chapter 4.2.1, flooding composition. All experiments were carried out at ambient temperature.

Figure 4.8. Gilson 222 XL Liquid Handler

First the core was flooded with several pore volumes of SW-U brine with a relatively high rate. This is a method to get the adsorbed sulfate from the rate optimalistion experiments out of the core. A sample of the effluent was sampled. Some barium was added into the solvent to see if a reaction between sulfate and barium would blacken the solvent. If a reaction happened, more brine without sulfate had to be flooded through the core. When all the sulfate were washed out of the core it was flooded with one pore volume of the same brine, SW-U, with the optimum rate 0.1 ml/min. It was carried out to gain chemical and pressure equilibrium inside the core. Then brine with sulfate could be flooded. First the core, 2-21, was flooded with SW-¼M with rate 0.1 ml/min. Fractions of the effluent were sampled by the Gilson fraction collector as shown in figure 4.8. The samples were diluted and filtered before both cation (Ca^{2+} and Mg^{2+}) and anion ($SO_4^{2-}$and SCN^-) concentrations were analyzed by the ion chromatograph.

The same process was repeated, except that the brines were changed. This time, after the core 2-21 was cleaned from sulfate, it was flooded with SW-½M brine. Samples of the effluent were analyzed. The relative concentration versus pore volume was plotted to see if the sulfate concentration would have an effect to the active surface area. Plots are discussed and shown in chapter 5.2.2.

4.4 Adsorption experiments

4.4.1 Core determination

Before the adsorption experiments were carried out a core had to be chosen. The core needed to have an active surface area inside the core. The active water-wet surface area is of great importance. At this area there is a possibility for adsorption of ions. This area was measured by chromatographic studies, as described earlier.

Limestone core 20A was first analyzed, core information in table 4.3. This core was selected because it had the best results from the imbibition test, see chapter 5.1.3. The core had been washed as described in chapter 4.1.4. After the washing process it was saturated with SW-U brine. The core was flooded with SW-½M. Fractions of the effluent were analyzed with the ion chromatograph. Relative concentration versus pore volume was plotted. The area between the relative concentration curve of thiocyanate and the relative concentration curve of sulfate indicates the active surface area. Plot of the curves is shown in chapter 5.2.3.

Since core number 20A did not seam to have an active surface area it could not be used in the experiments. A new core had to be selected. Limestone core 46A was chosen. It was saturated with SW-U. Information about the core is listed in table 4.3. This core was very like core 2-21 in color and looked homogenous. The active surface area in core 46A was measured by the same method as for core 20A and 2-21. The relative concentration of the two anions was plotted against pore volume, shown in chapter 5.2.3. This time there was as delay of the relative concentration curve of sulfate, which indicated an active surface area. Limestone core number 46A was selected to be the core used in the adsorption experiments.

After core 46A was decided to be the experimental core for the main adsorption experiments it was flooded with several pore volumes of distilled water. This was accomplished to get the salts out of the core. When only distilled water was inside to core it was placed inside a heating cabinet to evaporate the water out of the core. At a stable core weight the core was cooled and saturated with SSW brine.

4.4.2 Adsorption experiment

In the adsorption experiments the same setup as described in chapter 4.2.1, flooding composition, with some modifications, was used. The Hassler cell was placed inside a heating cabinet, so the temperature could be regulated. This is shown in figure 4.9. Another modification was that a backpressure valve was attached. This pressure was approx 7 bar. This pressure was added to prevent boiling inside the core since the temperature inside the heating cabinet would be as high as 130°C.

20°C

The SSW saturated core, 46A, was placed inside the Hassler cell in the heating cabinet. The first experiment was carried out at 20°C. SSW brine was flooded trough the core with a relatively high rate, 1.0 ml/min. Two pore volumes were flooded.

Figure 4.9. Heating cabinet

After the two pore volumes were flooded, the rate was lowered. The core was flooded (SSW) at rate of one pore volume per day. One pore volume per day was approx 0.01 ml/min. The Gilson sampler was programmed to sample fractions of the effluent. These samples were analyzed by the ion chromatograph. This giving relative concentration curves for sulfate, magnesium and calcium were plotted versus pore volume. Plots are shown in chapter 5.3.1.

130°C

After the ion adsorption experiment at 20°C was finished, the heating cabinet was heated to 130°C while there still was some SSW flooding through the core. When the temperature was reached and stable, at 130°C, two pore volume of SSW was flooded through the core by 1.0 ml/min. Then SSW was flooded through the core at one pore volume per day, 0.01 ml/min. The same limestone core was used at all the different temperatures, core 46A. The effluent was sampled, and analyzed. Relative concentration versus pore volume plots are shown in chapter 5.3.4.

100°C

When the absorption was measured at 130°C the temperature inside the heating cabinet was lowered to 100°C. The exactly same procedure was carried out at 100°C as for 130°C and 20°C. Relative concentration versus pore volume plots are shown in chapter 5.3.3.

80°C

After the adsorption at 100°C was analyzed the same procedure was carried out 80°C. Relative concentration versus pore volume plots are shown in chapter 5.3.2.

4.4.3 Active surface area

After the adsorption experiments were finished, a new active surface area test was carried out on core 46A.

The same procedure as described earlier was used. Limestone core 46A was flooded with several pore volumes of SW-U with a relatively high rate. Another pore volume was flooded through the core but with the experimental rate, 0.1 ml/min, to gain chemical and pressure equilibrium. Afterwards SW-½M was flooded through the core with a rate of 0.1 ml/min. Fraction of the effluent was sampled and analyzed. Plot and area are shown in chapter 5.2.4

4.4.4 Spontaneous Imbibition test

After the active surface area was analyzed the core was flooded with several pore volumes of distilled water to remove the salt form the core. The core was dried in a heating cabinet. At a stable weight it was cooled down and saturated with heptane. The 100% heptane saturated core was then placed inside an Amott cell together with the imbibition fluid, SSW. The imbibition cure is shown in chapter 5.2.5.

5 Results and discussion

The results from the reported experiments are discussed in this section. The different cores used were 12D, 20A, SK, 2-21 and 46A.

5.1 Spontaneous Imbibition

As described in chapter 4.1.3 three carbonate cores were placed in Amott cells to spontaneous imbibe and give an indication of the wettability of the cores. Core 12D, 20A and SK were used in these experiments.

5.1.1 SK

A Stevns Klint chalk core was spontaneous imbibed simultaneously as two limestone cores. The chalk core should be a collation between the two different types of carbonate. This chalk is known to behave water-wet. The core with a permeability about 2-3 mD (Zhang et al, 2005b. Austad et al, 1997) was saturated with heptane. Figure 5.1 shows the recovery curve of the chalk core. The plot shows that the heptane was produced quite rapidly. After the first day of imbibition, the recovery has almost reached its maximum. This is more clearly shown in figure 5.2.

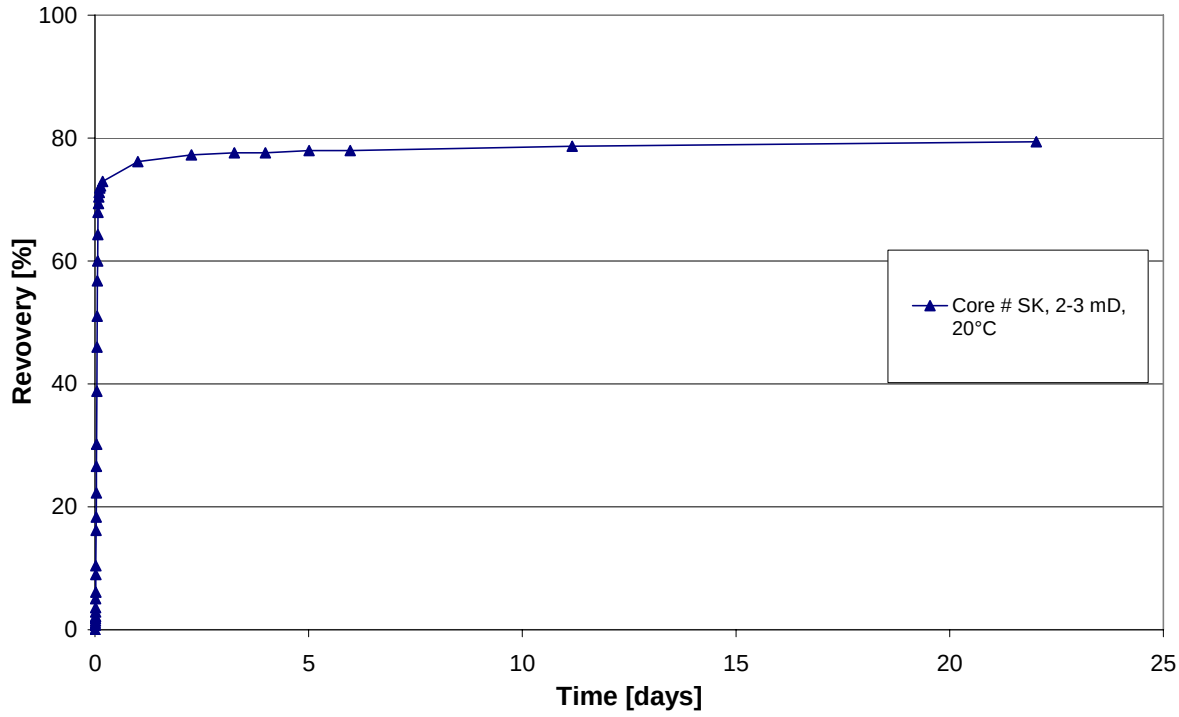

Figure 5.1. Recovery curve. Chalk core number SK.

Several parameters indicate that the SK core is wet-wet. The recovery is quite high; almost 80 percent of the original heptane in place has been produced. The high recovery gives a high increase in water saturation, ΔS_{ws}. This increase in water saturation is described in figure 3.11. A high ΔS_{ws} will give a high Amott water index, I_w. An exact value is not known since the other saturations in equation 3.7 are not known.

A common method to decide whether the spontaneous imbibition is dominated by gravity or capillary forces is to analyze the shape of the recovery curve. When it is curved, main driving mechanism is the capillary. If the curve is linear, the main driving force is gravity dominated. Figure 5.2 shows that the slope of the graph at the two first hours is relatively steep. The graph is also a bit curved; witch indicates that the imbibition force is mostly dominated by the capillary forces. The curve was expected to be more curved though. This may be caused by the adsorption of heptane on the glass surface in the Amott cell. However, the steep slop is an indication of the acting capillary pressure. The capillary pressure is dependent of the contact angle, θ. This angle indicates whether the wettability of a solid is water-wet or oil-wet, shown in figure 3.10.

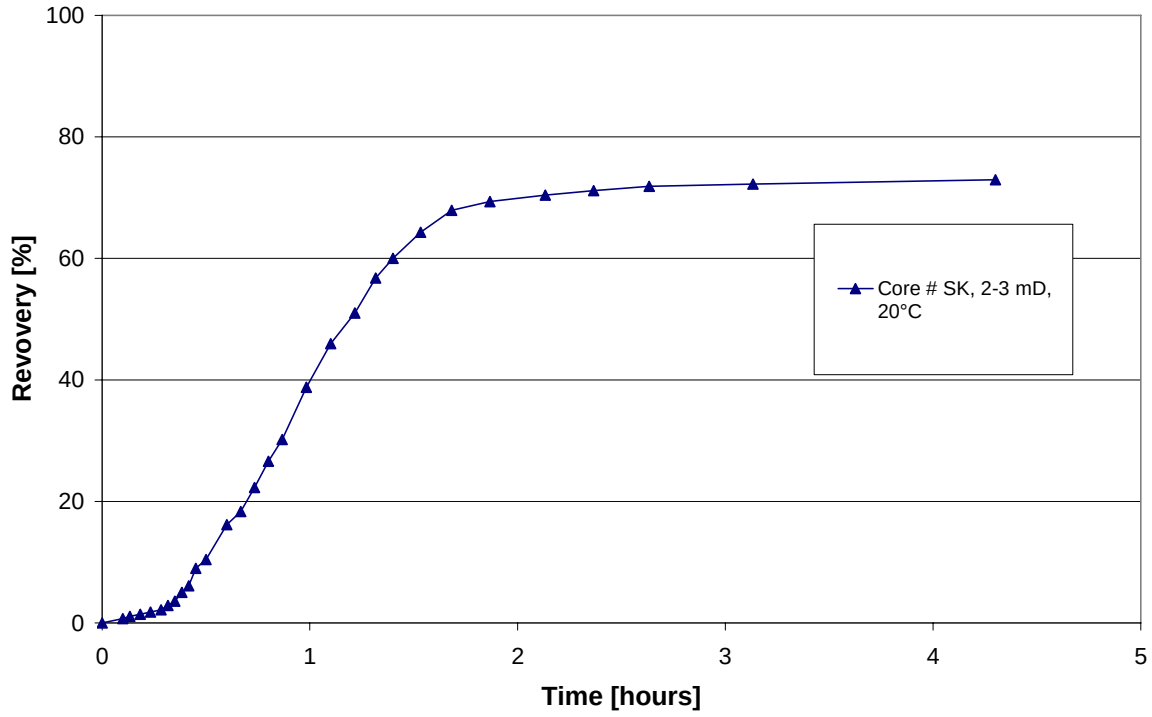

Figure 5.2. Recovery curve, the five first producing hours. Chalk core number SK.

After 2 hours, the slope of the graph in figure 5.2 flattens out and becomes almost linear. This change in the curve indicates that the capillary force is not the main imbibition force, but the gravity force. The gravity force has affected the production the entire production time, all though it has not been clearly seen because it is quite ineffective compared to the capillary force. Since this force is quite ineffective, the recovery curve flattens and only a few percent of the OHIP get produced after the capillary force stops acting on the fluid inside the core. In this case, the recovery rises with about 10 percent.

5.1.2 12D and 20A

12D and 20A are two limestone cores with different permeability. 20A has got the lowest permeability, 3.03 mD. 12Ds permeability was 20.40 mD.

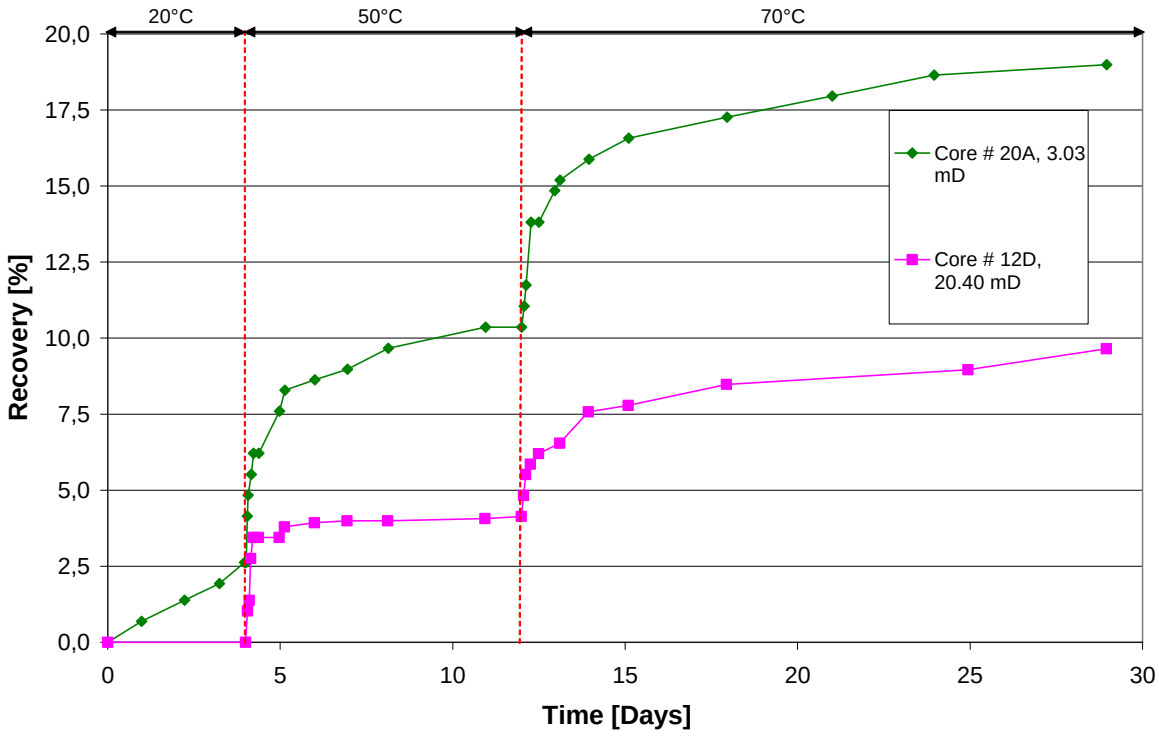

Figure 5.3. Recovery curves. Limestone cores number 20A and 12D.

Cleaned and dried cores have been saturated with 100% heptane, and put in Amott cells using SSW as the imbibition fluid. Figure 5.3 shows that the limestone cores have a low oil recovery after the first five days, at 20°C. 12D does not imbibe at all. This may be a sign that the core is oil-wet. 20A imbibes to a certain degree, only 2.5% oil recovery, but the imbibition is probably caused be the density differences of the two fluids, gravity forces. SSW has got a

higher density than heptane. The gravity force is the working force. Water-wet cores will have a potential for capillary forces. This can be explained by formula 3.4. A water-wet core has got a contact angle, less than 90°. This angle will give a positive capillary pressure. As described in chapter 3.1.3, a positive capillary pressure may cause spontaneous imbibition. If the core is oil-wet, $\theta > 90°$, the capillary pressure is negative. The more oil-wet the core is, the higher the contact angle becomes, which will lead to a higher negative capillary pressure. This negative capillary pressure may be powerful enough to prevent recovery from gravity forces. However, it seems from figure 5.3 that core 12D is in the oil-wet region since the core does not produce any oil. The negative capillary pressure is stronger than the gravity force. Negative capillary pressure in carbonates is quite common according to Høgnesen et al (2005). 80-90% of the worlds carbonate reservoirs are preferentially oil-wet.

After 4 days the Amott cells were placed in a heating cabinet at 50°C. This was carried out to speed up the imbibition process. Both cores show a rapid and small increase in oil production due to thermal expansion of the oil. Figure 5.3 shows that core number 20A to some degree is spontaneous imbibed by the capillary forces. Core 12D on the other hand shows no significantly increase in recovery after the thermal expansion.

After 12 days the temperature was increased to 70°C. Thermal expansion caused a rapid increase in oil production for both cores. After the thermal expansion it seemed like both cores produced by capillary driven forces for about 3 days. Then after 15 days the production is mainly gravity dominated. The spontaneous experiments were ended after 29 days. Core 20A got the highest recovery, 19%, and in the spontaneous imbibition experiment the capillary pressure seemed to be positive.

Even though core 20A seems to be the most water-wet, it may not be right. Since both limestone cores are from the Thamama field they are different in pore structure. It is not know at what well and depths they are collected from. The capillary pressure that dominates spontaneous imbibition is dependent of several parameters. These parameters are described in chapter 3.1.3. But only the value of the contact angle can change whether the capillary pressure is positive or negative.

5.1.3 20A, 12D and SK

Figure 5.4 shows all three recovery curves plotted in the same plot. This plot shows clearly that there are some differences between the two types of carbonates. The chalk has got about four times as high recovery as the best producing limestone core even the chalk only was spontaneous imbibed at 20°C.

This may indicate that SK is more water-wet than the limestones. Even though capillary pressure is dependent of several parameters as described in chapter 3.1.3.1, the most important parameter for this case is the contact angle. From formula 3.4 show if the angle is small the capillary pressure may become relative high.

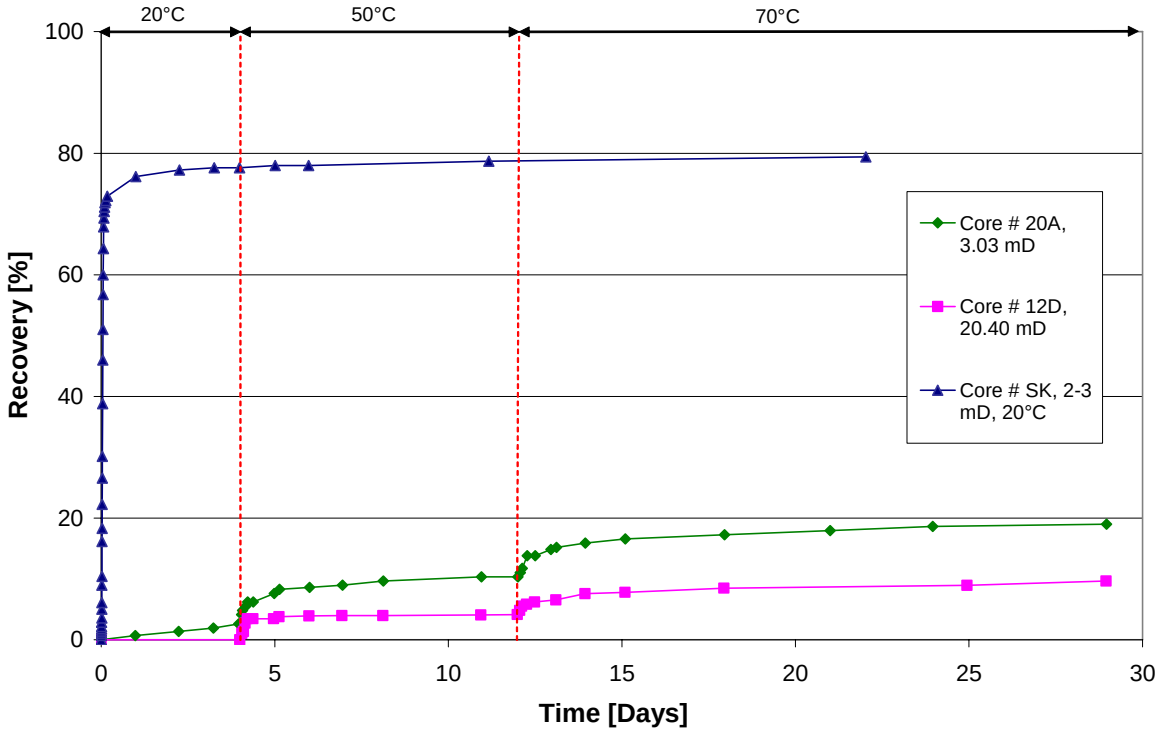

Figure 5.4. Recovery curve. Chalk core SK and limestone cores 20A and 12D.

A low recovery of the limestone cores was not unexpected. According to Hirasaki et al (2003) spontaneous imbibition in carbonates does not occur or is slow. The limestone cores are, as mentioned, from the Thamama field, but the SK core are from the Stevns Klint outcrop and not from a real reservoir. The low recovery also indicates that the core cleaning process, described in chapter 4.1.4 does not remove al the oil in the pores. The connection between the oil and the solids surface is strong. A chemical reaction is needed to change the wettability.

5.2 Chromatographic studies

The chromatographic separation of two water-soluble components, i.e. a tracer, SCN^-, and a potential determining ion toward carbonate, SO_4^{2-}, the fraction of the area covered by water represent the wetting index. The area between the effluent curves for SCN^- and SO_4^{2-} is proportional to the area contacted by water during the flooding process.

5.2.1 Rate optimization for limestone cores

Earlier chromatographic studies preformed on chalk have shown that an optimal rate was 0.2 ml/min (Strand et al, 2006). Table 4.1 shows that there are large differences in porosity between the two types of carbonates. Stevns Klint chalk has got porosity in the range 45-50%. The porosity of the limestone cores form the Thamama field used in this thesis is in the range of 24-27%.

Two rates were decided to be tested, first the optimal rate for Stevns Klint chalk experiment, 0.2 ml/min, and then 0.1 ml/min. Since the porosity of the limestone cores was approx half the value as the chalk, the rate was also divided by two. The rate with the most piston-like displacement of the core would be used through out the experiments. In this experiments core number 2-21 was used with a permeability of 2.70 mD, close to the chalk permeability.

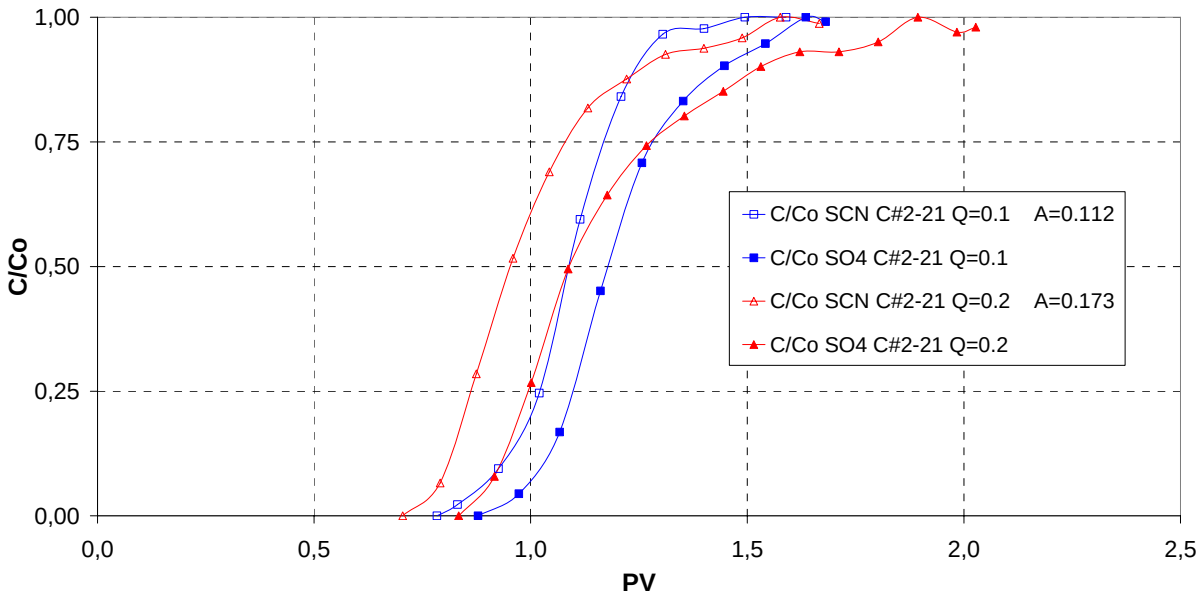

Figure 5.5. Rate optimization. Limestone core 2-21, SW-½M.

Figure 5.5 shows the relative concentration curves of both thiocyanate and sulfate versus pore volume. Most ideally the thiocyanate curve should cross C/C_0 equal to 0.5 at 1 pore volume injected and have the same symmetry at both sides of this cross point. This is an indication that the injected fluid is contacting the total pore volume of the core (Strand et al, 2006). The relative concentrations were measured by the Spectroquant photometer NOVA 60.

During the rate optimization with 0.2 ml/min, due to a failure in the fraction collector droplets of the effluent dropped on top of the fraction glasses. These droplets evaporated before the glasses were weight. So the curves at 0.2 ml/min in figure 5.5 should be a little bit flattened out and have the break through a bit later.

Area between the SCN^- curve and SO_4^{2-} curve indicates the active surface area, A_{wett}. This area is calculated as described in chapter 3.3.5. A rate of 0.2 ml/min had the largest adsorption area $A_{wett} = 0.173$; 0.1 ml/min gave an $A_{wett} = 0.112$ and was chosen as the optimum rate, due to the most piston like displacement of the core. This can be seen in figure 5.5, the slope of the thiocyanate curve is steep at the C/C_0 equal to 0.5 and the curve is symmetric at both sides of this cross point. The active surface area when flooding the core with a high rate is larger then when flooding with a low rate.

5.2.2 Effects of sulfate concentration

Previous studies preformed on chalk cores has shown that area between the SCN^- and SO_4^{2-} curves are dependent of the concentration of SO_4^{2-} in the injected brine (Strand et al, 2006). At low concentrations the area, at the same injection rate, was calculated to be the largest.

Limestone core 2-21 was flooded with two different brines, SW-¼M and SW-½M. The composition of these two brines is listed in table 4.2. The sulfate concentration is ¼ and ½ of the sulfate concentration in seawater respectively.

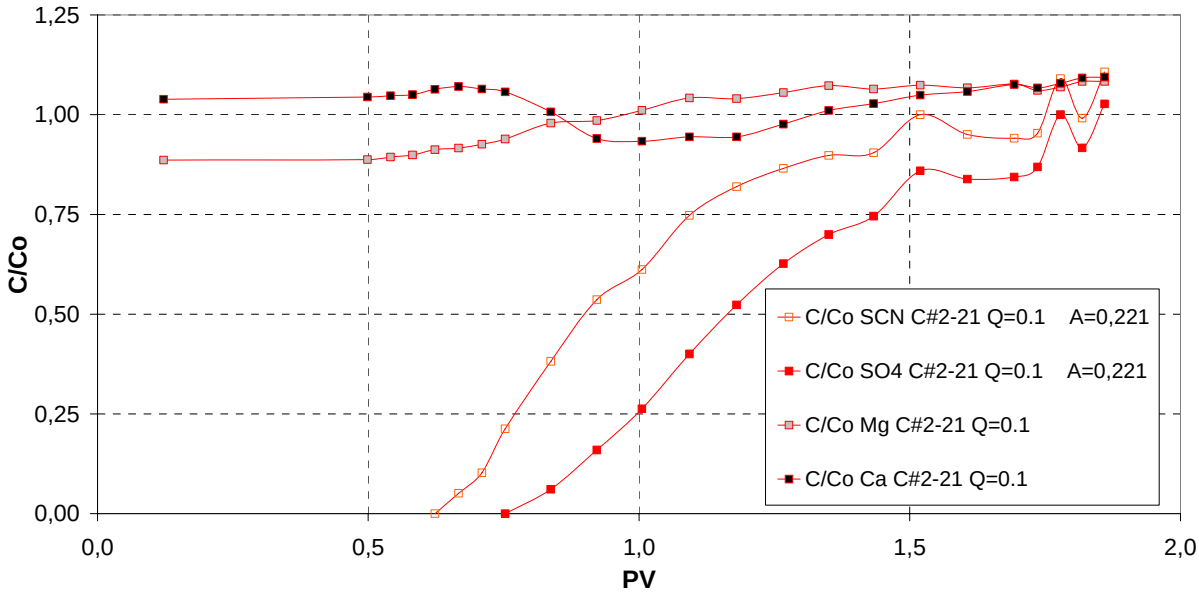

Figure 5.6. Chromatographic analyze. Limestone core 2-21, SW-¼M, Q=0.1 ml/min and ambient temperature.

Figure 5.5 and 5.6 show the relative SCN^- and SO_4^{2-} concentrations curves. These relative concentrations were measured by the Dionex ion chromatograph. The front of sulfate is delayed compared to the thiocyanate front; this is due to adsorption of sulfate. This indicates that there is an active surface area inside the core. The sensitivity of the sulfate ion regarding the surface charge on limestone is clearly demonstrated in figure 5.5 and 5.6

Flooding the core with SW-¼M gave an area between SCN^- and SO_4^{2-} curves, A_{wett}, equal 0.221, while flooding core 2-21 with SW-½M gave an area equal 0.151. The limestone cores behaves as the chalk cores studied by Strand et al (2006). An increased area with decreasing

sulfate concentration in the injection brine indicated that the delay is due to sulfate adsorption. Strand's studies showed an area in the range of 0.25 to 0.23 with sulfate concentration, of 0.012 mole/l. With a sulfate concentration of 0.024 mole/l an area between the two anion curves was calculated to be in the range of 0.168 and 0.171. There are of course some uncertainties; two different concentrations have been used. However, the same trend is present in both types of carbonates, an increase in the area when the sulfate concentration in brine is decreased. The experiments also confirm that for a limestone core with small PV chromatographic separation of SCN^- and SO_4^{2-} is large enough to determine the area between the effluents curves.

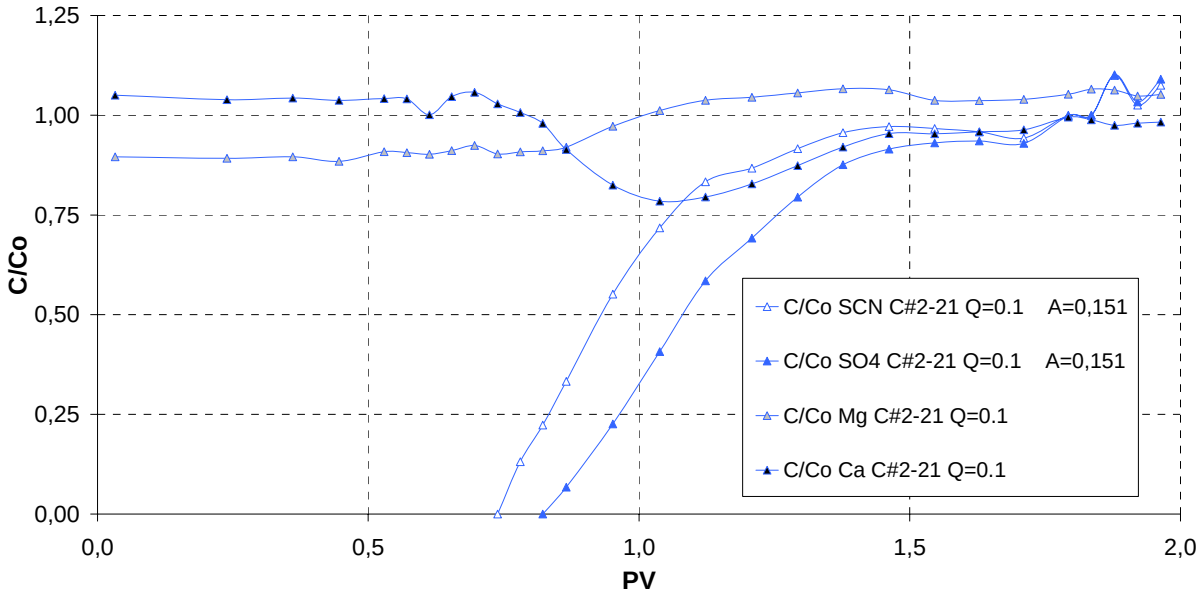

Figure 5.7. Chromatographic analyze. Limestone core 2-21, SW-½M, Q=0.1 ml/min and ambient temperature.

Figure 5.6 and 5.7 also shows the relative concentrations of the two cations, magnesium and calcium. Both figures show that the gradient of the sulfate concentration in the dispersion zone caused a change in the Ca^{2+} concentration. As the sulfate concentration increase, sulfate adsorbs onto the limestones surface. This adsorption of sulfate will reduce the positive surface charge. This will change the equilibrium condition for the strongly potential-determining Ca^{2+}-ion, causing the Ca^{2+}-ions to adsorb onto the surface. The continuous supply of injection fluid will then re-establish equilibrium between ions in solution and adsorbed material. The minimum in calcium concentration is shown in figure 5.6 and 5.7 to be close to the inflection point of the sulfate effluent curve. The change in the Ca^{2+} concentration is closely related to

the dispersion zone of sulfate. This has also been shown in chromatographic studies of chalk (Strand et al, 2005).

Studies preformed on chalk did not show any major variations in the Mg^{2+} concentration at ambient temperatures (Strand et al, 2006). The chromatographic studies preformed on limestone on the other hand shows some variation. Probably is this difference caused by the two different measure techniques. The limestone experiments were analyzed by an ion chromatograph. The accuracy of this instrument is very high and denotes small variations in the concentrations. Analyses preformed using chalk gave no good indication of the variation of Mg^{2+}-ions due to almost 4 times higher Mg^{2+} concentration than calcium in SSW.

Figure 5.6 and 5.7 show that as the calcium concentration decreases as the magnesium concentration increases. When SW-U, containing magnesium and calcium ions, was flooded through the core equilibrium of magnesium and calcium was established. The affinity of calcium is higher than the affinity of magnesium, but the brine consists of almost four times as high molecular concentration of magnesium ions as calcium ions. The exact amount is 0.045 mole/l magnesium ions and 0.013 mole/l calcium ions. This high concentration of Mg^{2+}-ions inside the core before injecting brine containing sulfate makes the increase of magnesium concentration. When sulfate is adsorbed, calcium ions become the most dominating potential-determining ions. This can be seen in figure 5.6 and 5.7. The change in Mg^{2+}-ion concentration is closely related to the dispersion zone of sulfate. Mg^{2+}-ion concentration increases as the Ca^{2+}-ion decreases and SO_4^{2-} is adsorbed to the surface inside the core.

5.2.3 Selection of cleaned limestone cores.

Before the main adsorption experiments could start, a core with an active surface area had to be chosen. Limestone core 20A was investigated. This core was the limestone core with the highest recovery from the spontaneous imbibition experiments.

Core 20A was chromatographic tested with SW-½M. Figure 5.8 shows the relative concentration of both anions (SCN^-, SO_4^{2-}) and cations (Mg^{2+}, Ca^{2+}). The separation between the non-potential determining ion thiocyanate and potential determining ion sulfate indicates that the active surface area does almost not exist. It is calculated to be 0.015. Figure 5.8 shows that there are almost no separation between SCN^- and SO_4^{2-}. The calcium concentration decreases at the separation of sulfate and thiocyanate and the magnesium concentration increases. This is caused by the same mechanism as discussed in chapter 5.2.2. But the increase and decrease in cations is not as significantly as for core 2-21. This is illustrated in figure 5.8.

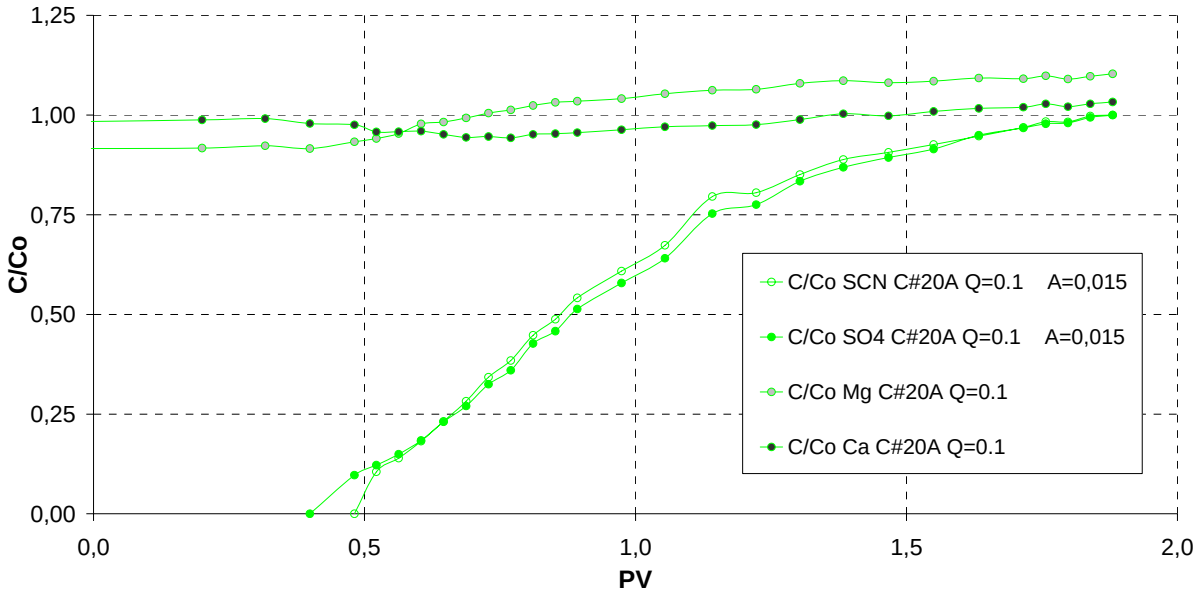

Figure 5.8. Chromatographic analyze. Limestone core 20A, SW-½M, Q=0.1 ml/min and ambient temperature.

The comparison of limestone core 20A and 2-21 shows a major difference in the active surface area. The active surface area, A_{wett}, inside 20A is just a tenth of the active surfaces area inside 2-21, 0.015 and 0.151 respectively. This indicates that the core is still oil-wet after cleaning with toluene and methanol. This can also be the reason why the recovery of core

20A, measured in the spontaneous imbibition experiments, was so. However, another major difference between the two cores was the piston like displacement. 2-21 showed good piston-like displacement, while 20A did not. This indicates that the limestone cores used in the experiments does not have the same pore distribution. Wettability and pore structures vary form core to core. The non-piston-like displacement of core 20A is probably caused by some high permeability zones through the core, and probably not cracks, since the relative concentration of thiocyanate almost cross 0.5 at 1 pore volume injected. This is an indication that the entire core has been swept.

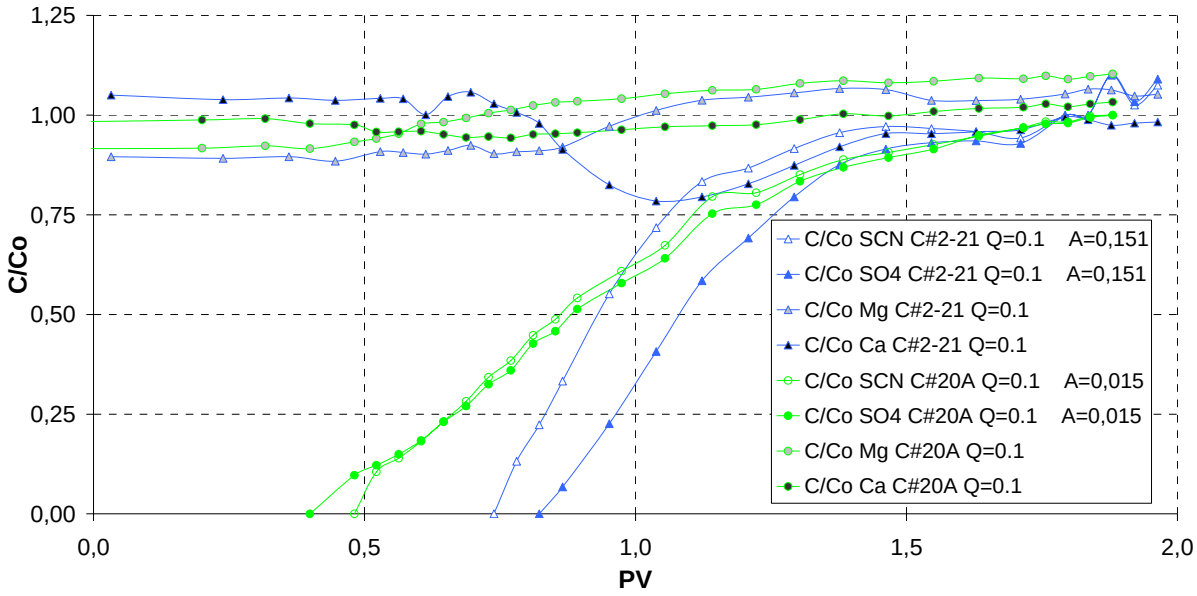

Figure 5.9. Chromatographic analyze. Limestone core 20A and 2-21, SW-½M, Q=0.1 ml/min and ambient temperature.

As described core 20A did not have the properties as wanted, a minor active surface area and non piston like displacement. A new limestone core was selected, 46A. This core was selected to the chromatographic studies because of its light colors and seemed homogeneous.

Chromatographic test of core 46A is shown in figure 5.10. The displacement of the core is piston-like. The relative concentration of thiocyanate crosses 0.5 at 1 pore volume injected, and the displacement sweeps the entire core. The active surface area is calculated to be 0.107. The calcium concentration decreases as the sulfate is adsorbed to the core, meanwhile the magnesium concentration increases. The increase of both the cations at 0.7 pore volume

injected is probably caused by an error when preparing the sample. Anyway, this core showed the properties acceptable and can be used in the adsorption experiments.

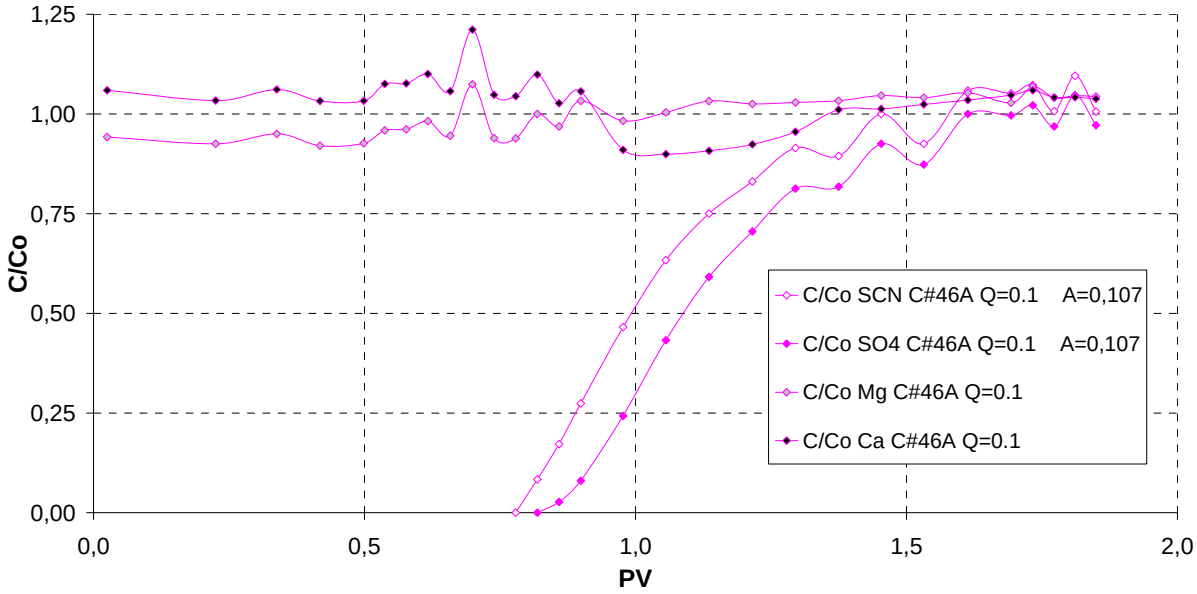

Figure 5.10. Chromatographic analyze. Limestone core 46A, SW-½M, Q=0.1 ml/min and ambient temperature.

5.2.4 Cleaning of limestone cores with SSW at high temperature

The core was cleaned by injection of seawater with a low injection rate. After the core was flooded with SSW at 130°C at a low rate, a new chromatographic test was performed on limestone core 46A. Figure 5.11 shows the result of this test.

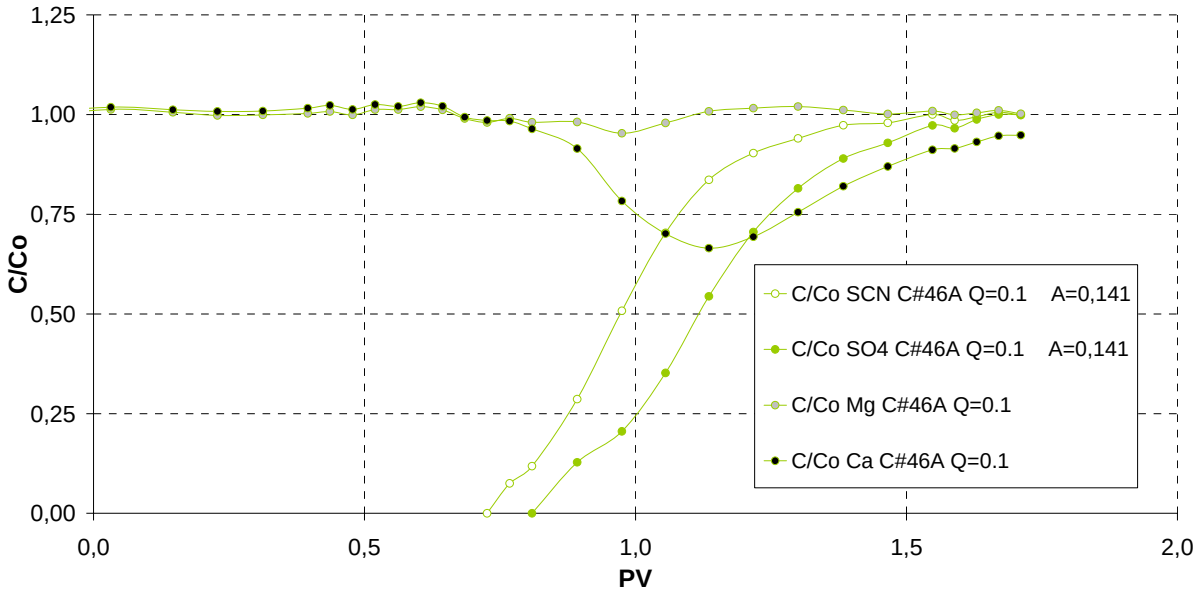

Figure 5.11. Chromatographic analyze after substitution at 130°C. Limestone core 46A, SW-½M, Q=0.1 ml/min and ambient temperature.

The active surface increased. The adsorption area increased with 32%, from 0.107 to 0.141. Figure 5.12 show the chromatographic analyses before and after the adsorption test at 130°C. Another major difference from the two chromatographic tests was the sensitivity of calcium. The adsorption of calcium increased drastically. After flooding with SSW at high temperatures the active surface area increases and makes more room for adsorption of calcium ions as the sulfate is adsorbed.

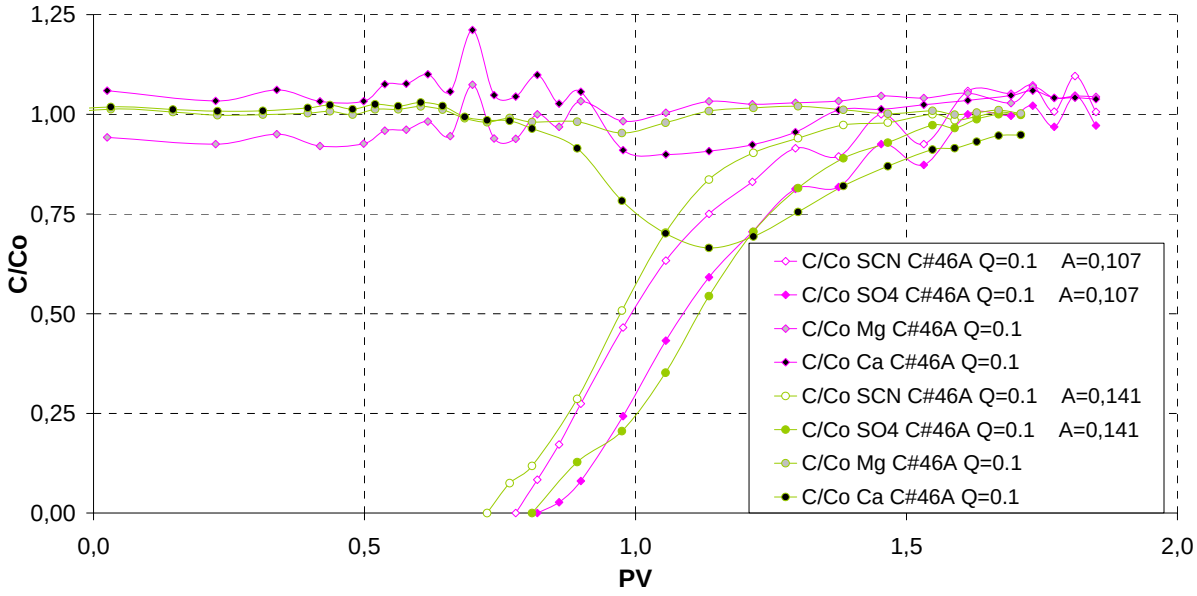

Figure 5.12. Chromatographic analyze before and after substitution at 130°C. Limestone core 46A, SW-½M, Q=0.1 ml/min and ambient temperature.

5.2.5 Spontaneous imbibition after substitution at 130°C

Core 46A was cleaned with distilled water, several pore volumes were flooded and salt was removed. The core was placed in a heating chamber and evaporated the remaining fluids. The core was saturated with heptane and placed in an Amott cell.

Figure 5.13 shows the recovery of core 46A. The production of this core was very much like the production as for the two other imbibed cores, 12D and 20A. The main production started when the temperature was increased to 70°C. A rapid increase in the recovery is probably caused by the capillary forces. They are more active as the temperature increases.

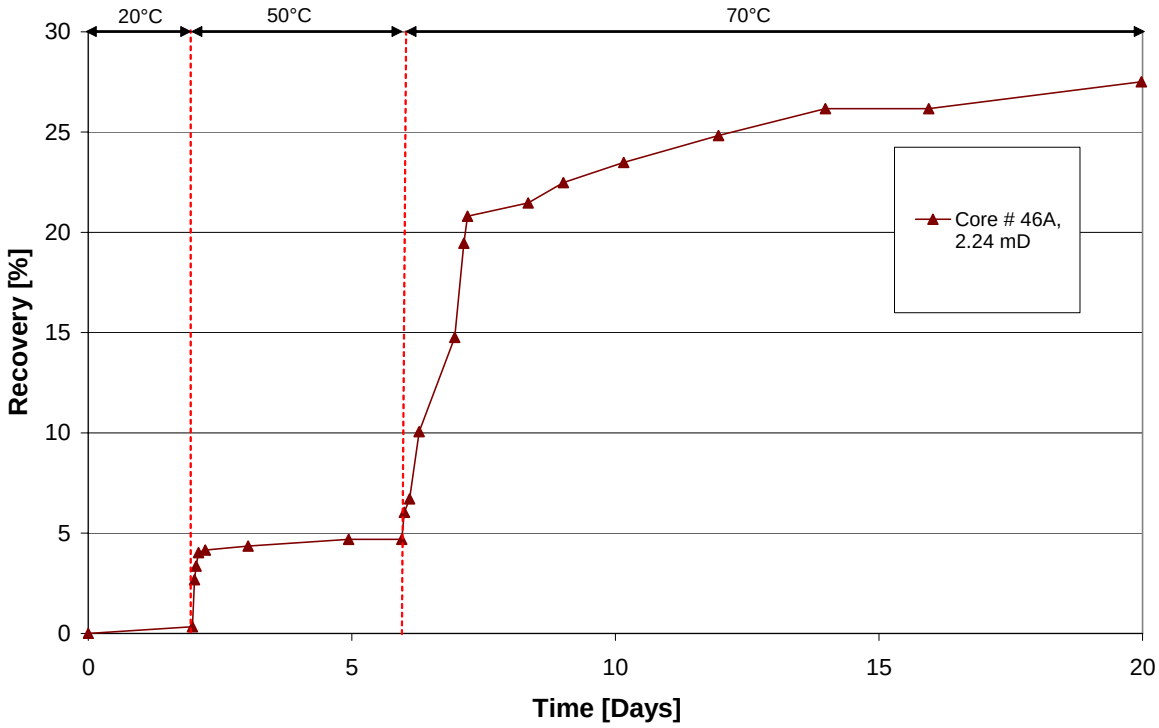

Figure 5.13. Recovery curve. Limestone cores number 46A.

The main difference between the first two cores (12D and 20A) and 46A is the recovery. 46A has a higher recovery. 20A, who reached the highest recovery, 19%, in the pre-experimental test has got a significantly lower recovery than 46A. Core produced 28% of the original oil in place. Both cores have approx the same permeability. The difference may be caused by either the difference in initial wetting conditions of the cores or that the increase of active surface area has increased and made the core more water wet.

5.3 Adsorption experiments

The toluene/methanol cleaned limestone core 46A was used in the adsorption experiments. Seawater, SSW, containing seawater concentration of potential determining ions (Mg^{2+}, Ca^{2+} and SO_4^{2-}) was flooded very slowly, 1 pore volume per day, through the limestone core at various temperatures, 20°C, 80°C, 100°C and 130°C. Fraction of the effluent were analyzed by the ion chromatograph and relative concentrations of the potential determining ions were plotted versus pore volume injected.

5.3.1 20°C

Figure 5.14 shows that at 20°C no significantly changes in the relative concentration of the potential determining ions were measured. Studies preformed on chalk indicated the same, no substitution of either magnesium or calcium (Korsnes et al, 2006).

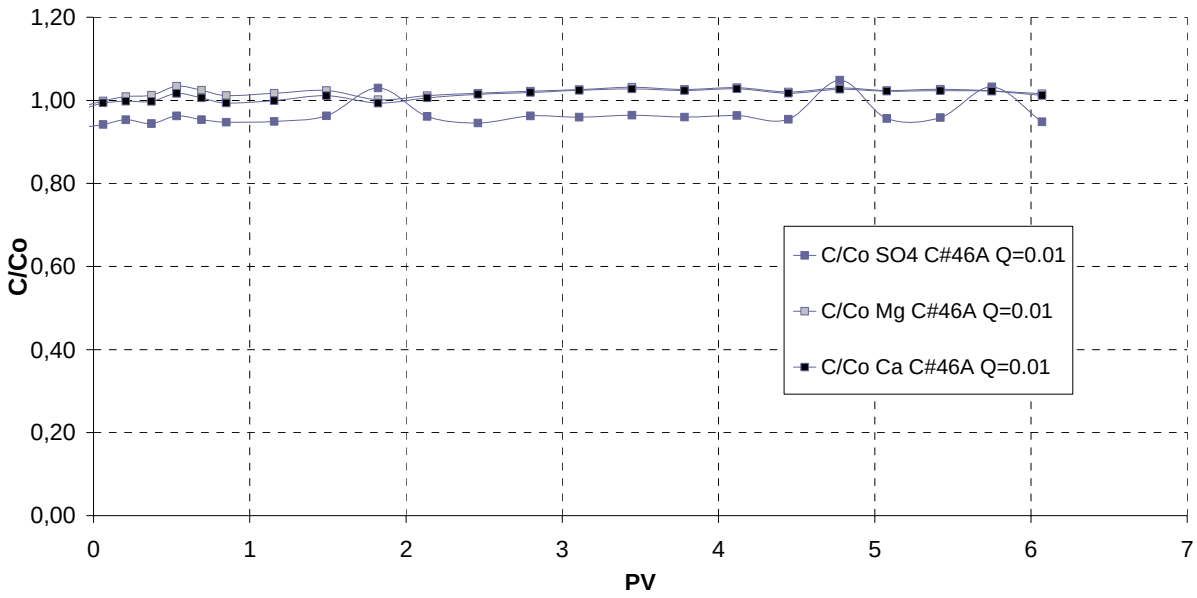

Figure 5.14. Relative concentration of potential determining ions at 20°C, core # 46A, SSW and Q=0.01 ml/day.

Figure 5.15 shows that no substitution or adsorption occurs. The dotted lines are the molecular concentration of potential determining ions in the initial fluid. All the three potential determining ions have got the same concentration as the initial injected fluid. Calcium is close to 0.013 mole/l, magnesium close to 0.045 mole/l and sulfate close to 0.024

mole/l. There are just some minor changes, this are probably caused by the uncertainties in the preparation of the effluent samples.

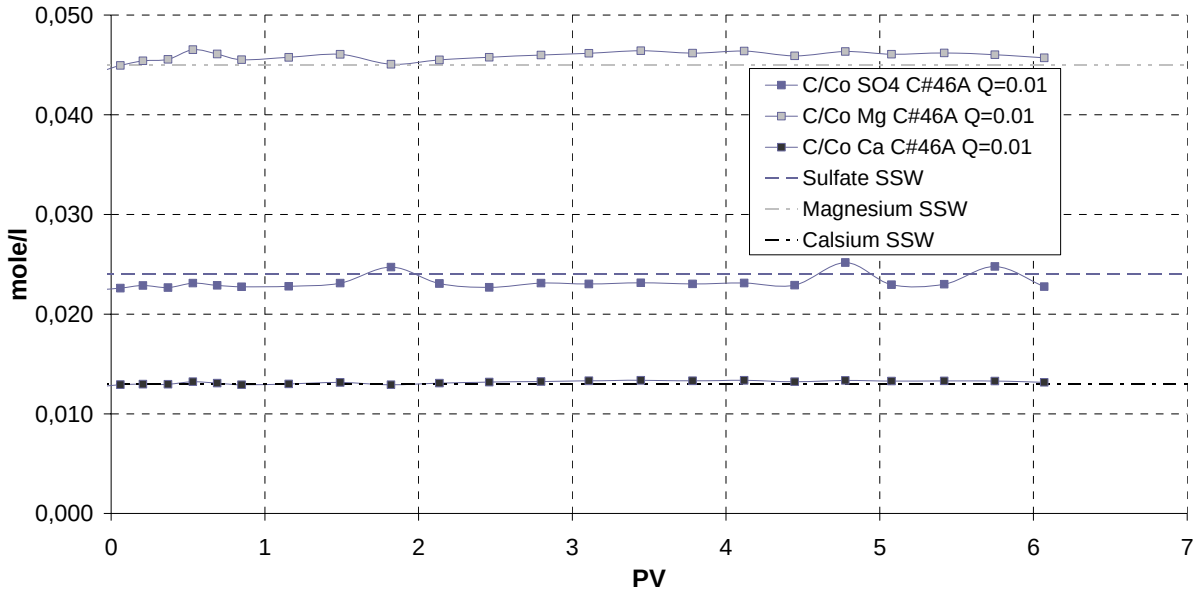

Figure 5.15. Molecular concentration of potential determining ions at 20°C, core # 46A, SSW and Q=0.01 ml/day.

5.3.2 80°C

While flooding the core at 80°C, shown in figure 5.16, the relative concentrations of the potential determining ions were stable. Studies preformed on chalk at 70°C by Korsnes et al (2006) have indicated the same, no major adsorption or substitution.

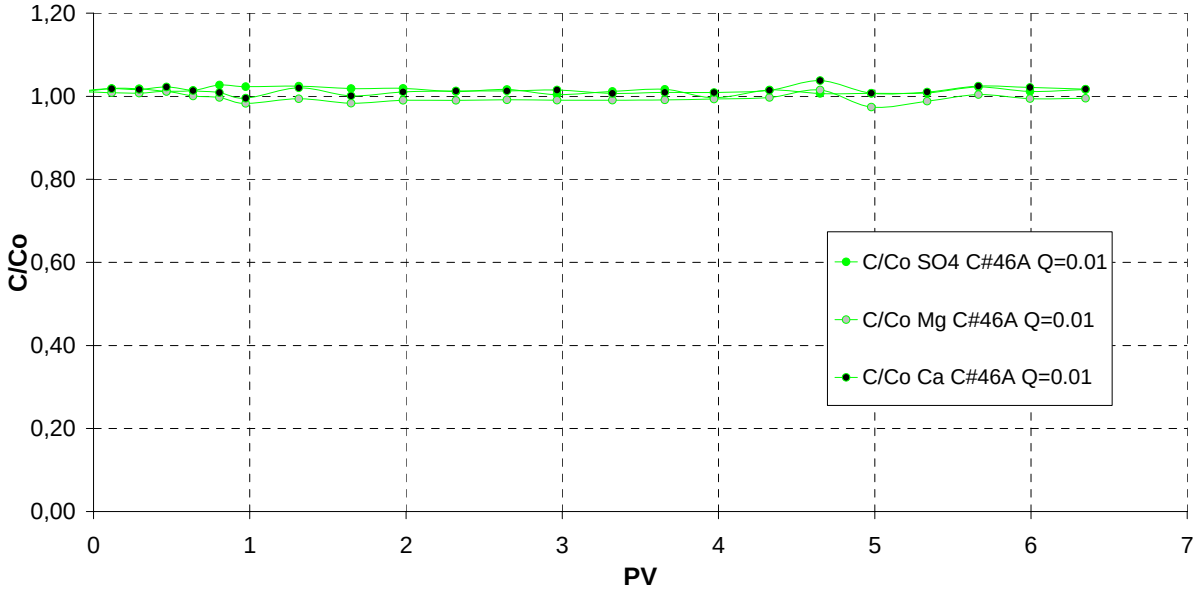

Figure 5.16. Relative concentration of potential determining ions at 80°C, core # 46A, SSW and Q=0.01 ml/day.

Figure 5.17 shows the same as for 20°C, no variations in the molecular concentrations of the potential determining ions.

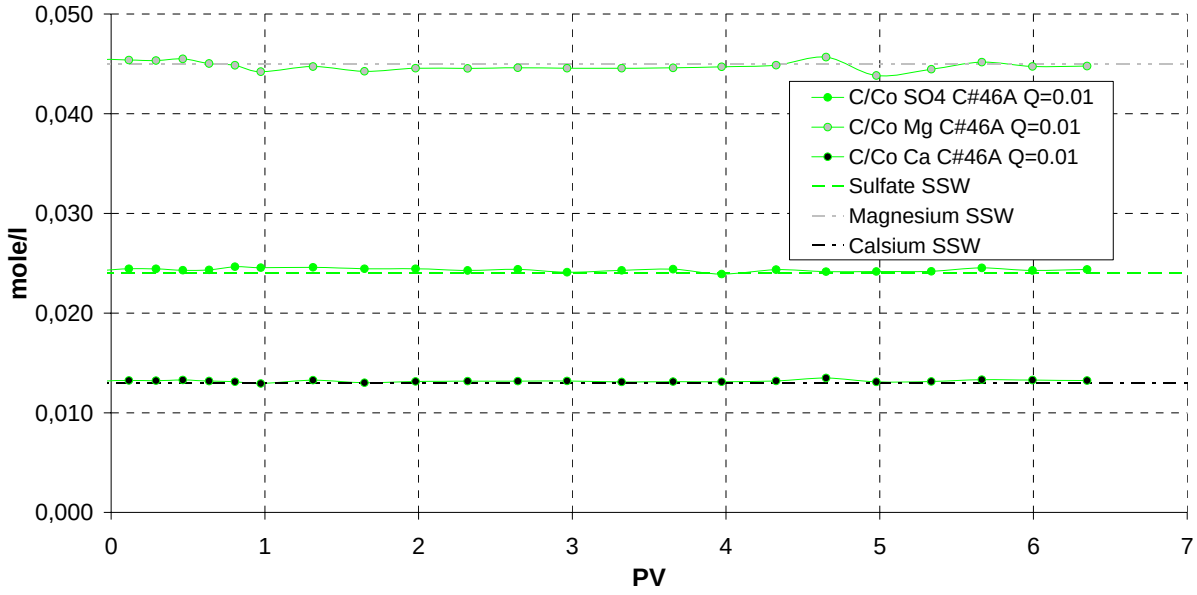

Figure 5.17. Molecular concentration of potential determining ions at 80°C, core # 46A, SSW and Q=0.01 ml/day.

5.3.3 100°C

When flooding core 46A with SSW at 100°C the relative concentration of magnesium and calcium decreased and increased, respectively. This is shown in figure 5.18. The potential determining ion sulfate was stable. Calcium increased at the maximum with 17%. The relative concentration became more or less stable after 3.5 pore volume injected. Magnesium decreased as calcium increased. The relative concentration of magnesium decreases by 4% from the injected fluid. This concentration seemed to be stable at the same point as calcium, approx 3.5 pore volume injected. This indicates a substitution of ions at the rock surface.

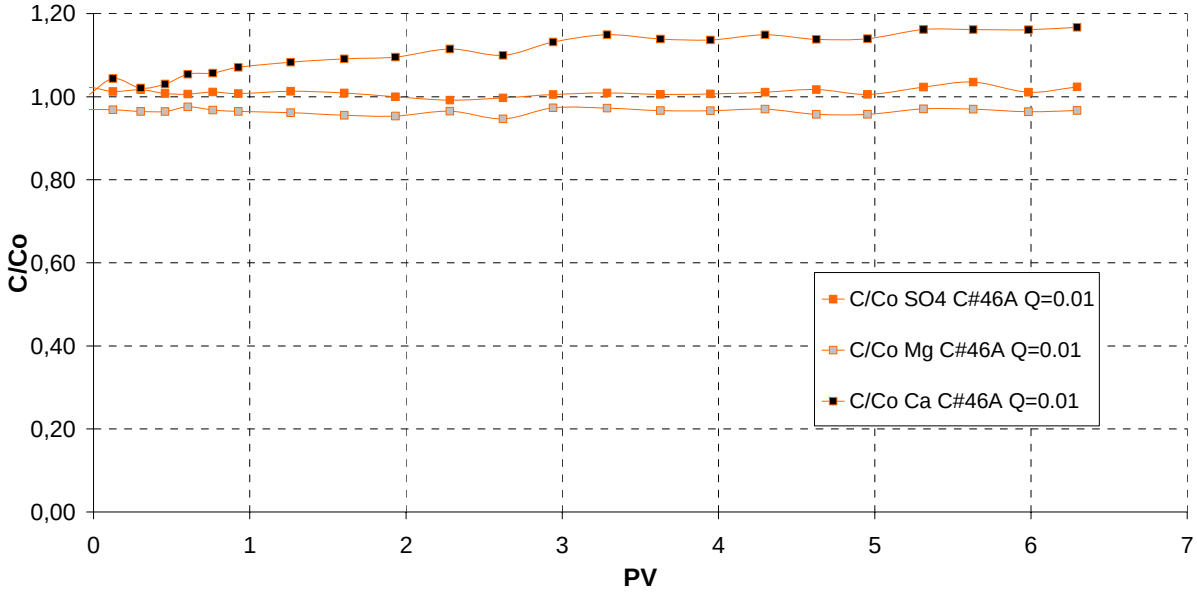

Figure 5.18. Relative concentration of potential determining ions at 100°C, core # 46A, SSW and Q=0.01 ml/day.

This substitution is more clearly illustrated in figure 5.19. This figure shows the relative concentrations in mole/l. As seen in figure 5.18 SO_4^{2-} is stable, no variations in the relative concentration. Mg^{2+} and Ca^{2+} concentrations clearly indicate that a substitution of ions occurs. This can be seen by the area between the relative concentration and the initial concentration is approx the same for both Mg^{2+} and Ca^{2+}. As Mg^{2+} adsorbs, Ca^{2+} is released form the surface. This causes the increase in calcium concentration and the decrease of magnesium concentration. The substitution continues for more than 6 PV, and could indicate that not only substitution of ions at the surface is taking place. Another explanation could be dolomitization shown in reaction 5.1

$$2CaCO_3 + Mg^{2+} \rightarrow CaMg(CO_3)_2 + Ca^{2+} \qquad 5.1$$

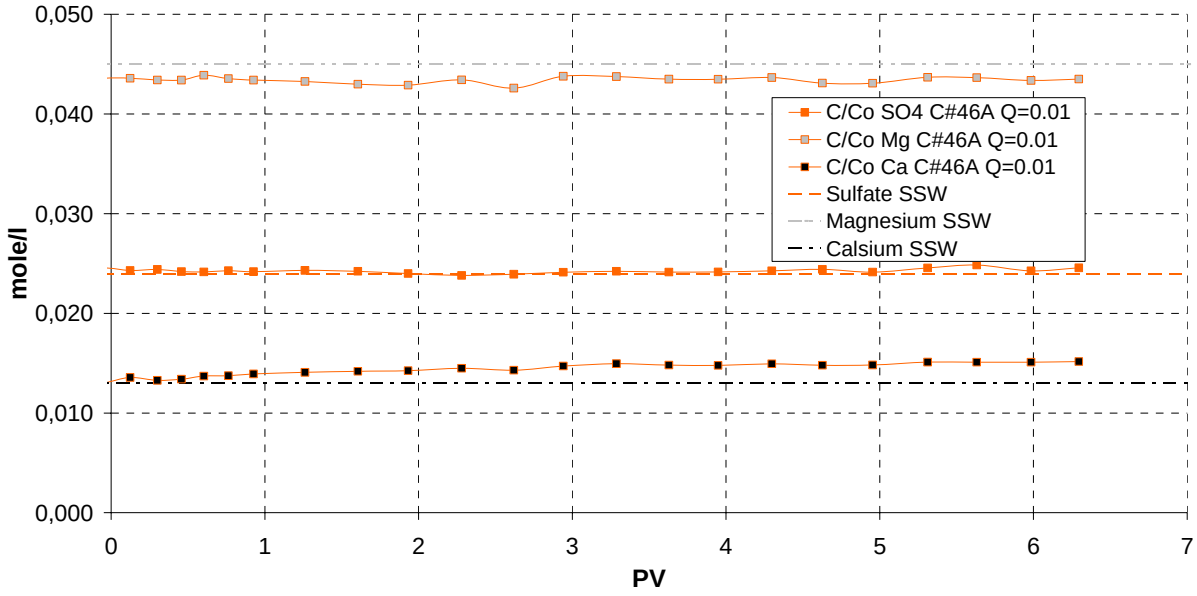

Figure 5.19. Molecular concentration of potential determining ions at 100°C, core # 46A, SSW and Q=0.01 ml/day.

5.3.4 130°C

When flooding the limestone core at 130°C the same phenomena occur as seen at 100°C. The main difference is that at 130°C the substitution occurs more rapid and with a larger number. Ca^{2+} concentration is more or less stable after just 1 pore volume injected. At 130°C the calcium concentration increases by 48% at its maximum. Magnesium on the other hand reaches a minimum of 15% less than the initial brine. No adsorption of sulfate is taking place at this temperature.

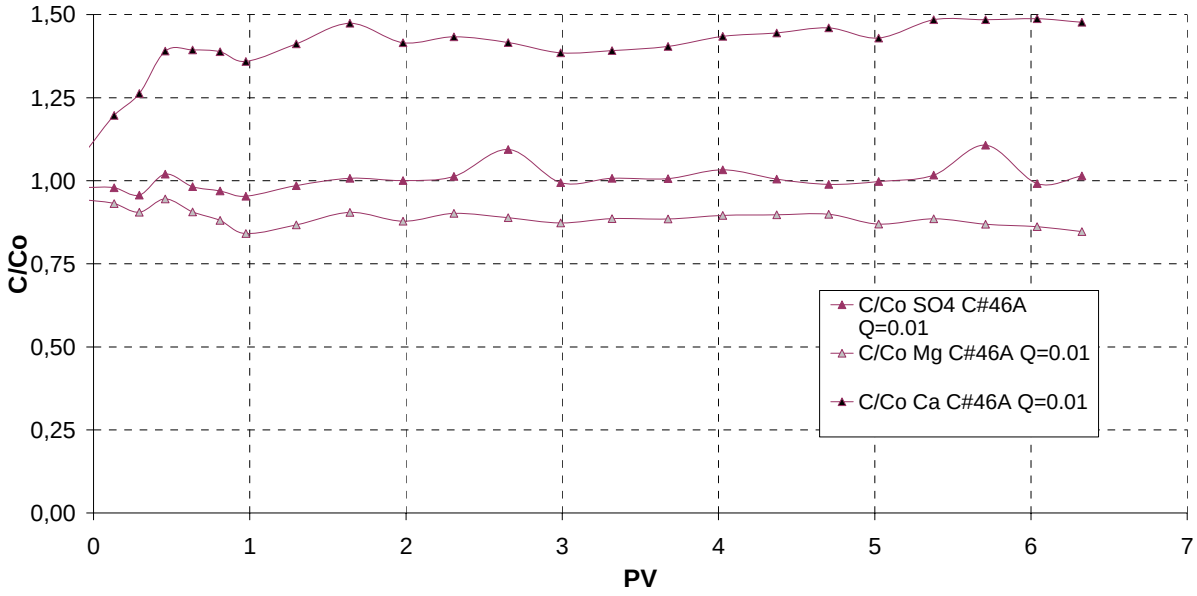

Figure 5.20. Relative concentration of potential determining ions at 130°C, core # 46A, SSW and Q=0.01 ml/day.

Figure 5.21 shows that the increase in molecular concentration of calcium is approx the same as the decrease in molecular concentration on magnesium. These changes indicates the same as mentioned at 100°C, magnesium ions is adsorbed to the surface inside the limestone core and is substituted by the by the same amount of calcium ions.

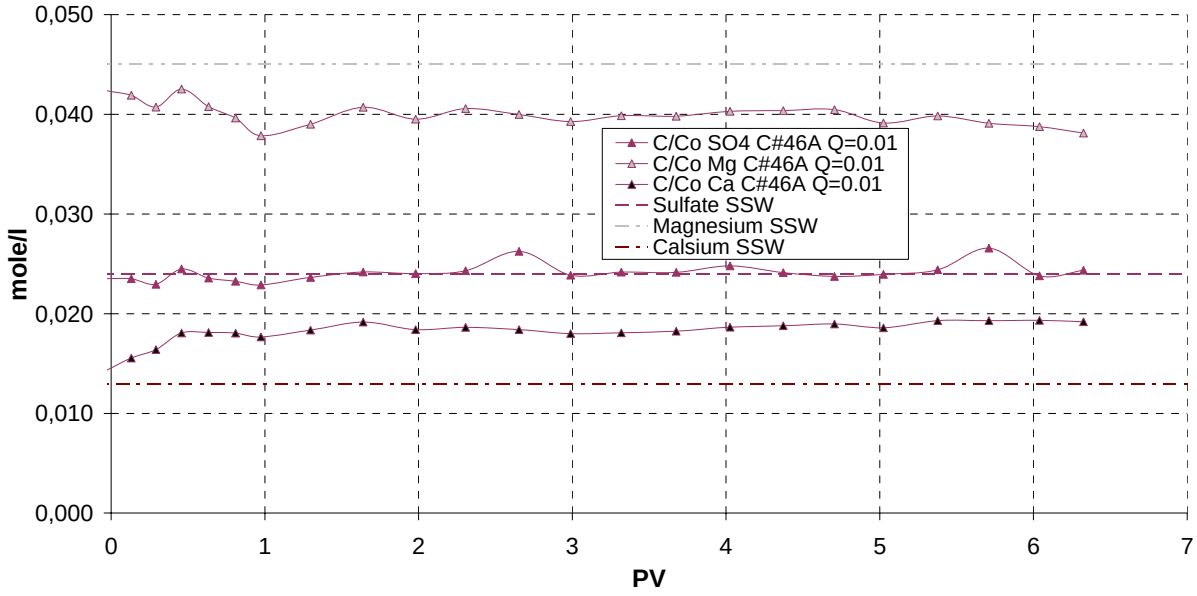

Figure 5.21. Molecular concentration of potential determining ions at 130°C, core # 46A, SSW and Q=0.01 ml/day.

5.3.5 Variations in magnesium concentration at different temperatures

Figure 5.22 shows the variations in relative concentration at the different experimental temperatures. At the two lowest temperatures, no major variations in the concentrations occur. First at 100°C the concentration decreases and magnesium ions are adsorbed inside the limestone core. Figure 5.22 also show that the adsorption is a function of temperature, the increase at 130°C is much higher than at 100°C.

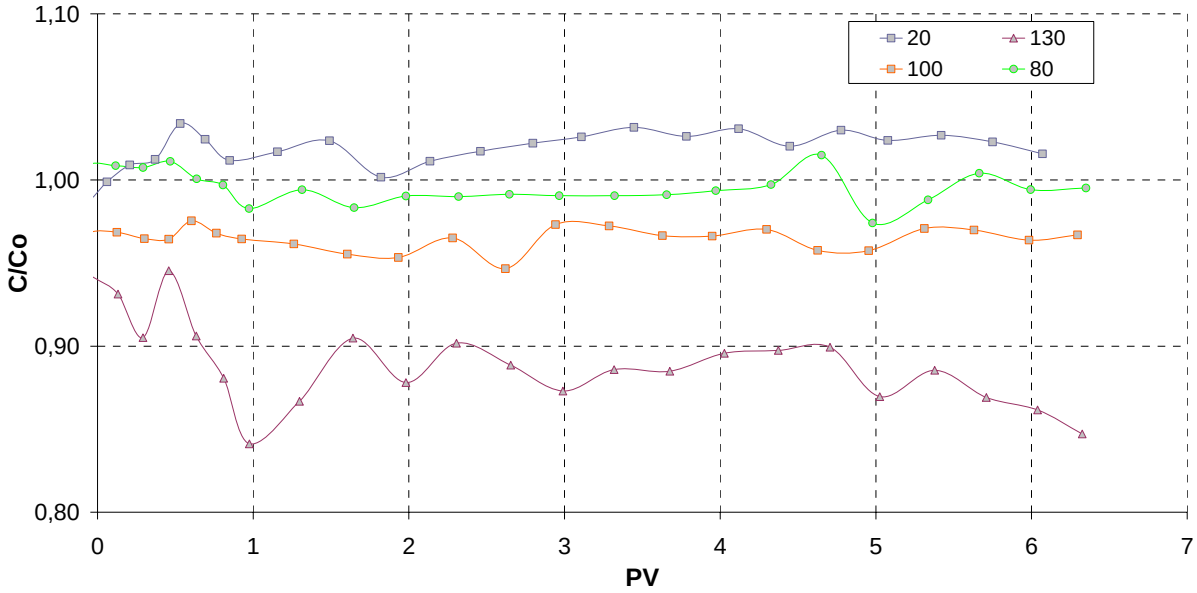

Figure 5.22. Relative concentration of the potential determining ion Mg^{2+} at the experimental temperatures, core # 46A, SSW and Q=0.01 ml/day.

5.3.6 Variations in calcium concentration at different temperatures

Figure 5.23 illustrates the same as figure 5.22. The substitution of potential determining ions is a function of temperature. The relative concentration of calcium ions is stable at the two lowest temperatures. At 100°C the concentration of calcium ions increases, but not as much as for 130°C. The substitution of ions increases as the temperature increases.

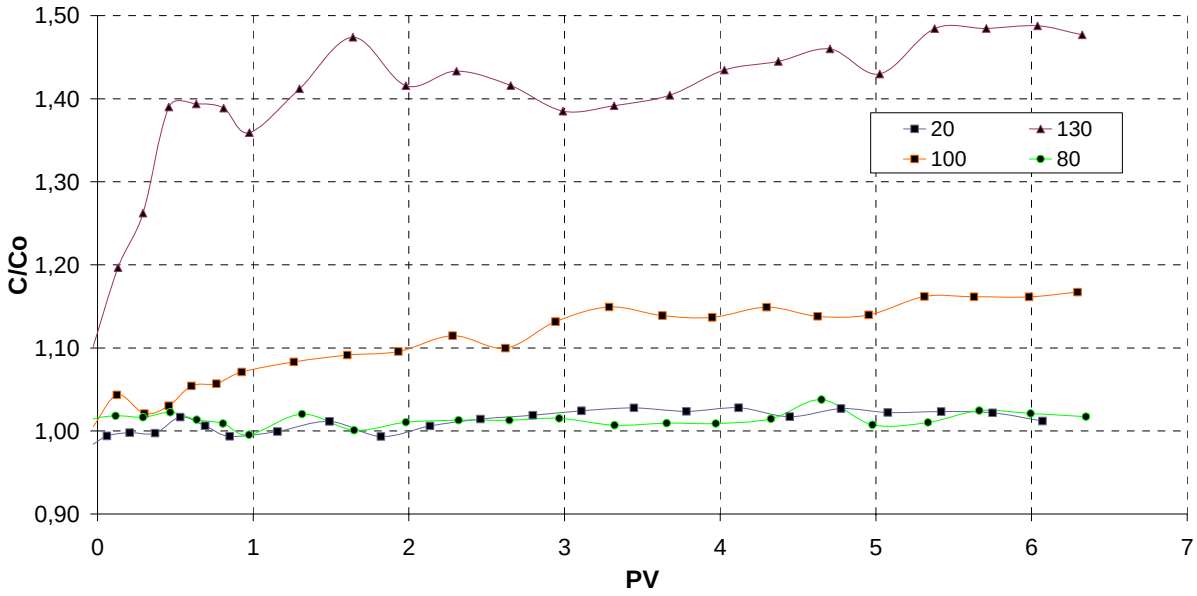

Figure 5.22. Relative concentration of the potential determining ion Ca^{2+} at the experimental temperatures, core # 46A, SSW and Q=0.01 ml/day.

6 Conclusions

From the experimental results in this project, the following conclusions can be drawn:

- Cleaned Thamama cores behaved oil-wet during spontaneous imbibition experiments.
- Chromatographic test can be used to determine whether or not an active water-wet surface is present in limestone core.
- Both concentration ½ and ¼ SO_4^{2-} had an acceptable adsorption surface area.
- Using SSW with ½ SO_4^{2-} concentration was the most practical concentration regarding chemical analyses.
- A substitution of the potential determining ions, calcium and magnesium, occurs at high temperatures (100°C and 130°C), when sulfate is present in injected fluid.
- The substitution of calcium and magnesium, when sulfate is present in injected fluid, increased the active water-wet surface inside the limestone core.

7 Future work

Suggestions to future work:

- Long time flooding of limestone cores with SSW at low rate to investigate if the substitution of calcium and magnesium is a dolomitization process.
- Can SSW be used for core cleaning of limestone cores? Investigate the change of spontaneous imbibition of a limestone core after substitution at 130°C. First spontaneous imbibe the core, then detect the active surface area and flood the core slowly (1 PV/day) with SSW at high temperature (130°C) over a long period of time. Measure the active surface area once more and than spontaneous imbibe the core.
- Investigate a correlation between increase in recovery by spontaneous imbibition and increase in active surface area.
- Investigate a correlation between active surface area and substitution of cations.

8 Symbols and Abbreviation

σ	Interfacial tension, mN/m
σ_{os},	Interfacial tension oil-solid
σ_{ws},	Interfacial tension water-solid
σ_{ow}	Interfacial tension oil-water
ρ	Density, kg/m^3
$\Delta\rho$	Density difference between oil and water, kg/m^3
Δp	Pressure across the capillary tube, Pa
ΔP_g	Pressure difference between oil and water due to gravity, Pa
ΔS_{os}	Increase in oil saturation during spontaneous imbibition of oil
ΔS_{ot}	Total increase in oil saturation during spontaneous and forced imbibition of water
ΔS_{ws}	Increase in water saturation during spontaneous imbibition of water
ΔS_{wt}	Total increase in water saturation during spontaneous and forced displacement of oil
μ	Viscosity, cP
θ	Contact angle, °
ϕ	Porosity, fraction or %
Ø	Diameter, cm
A_1	Area under the secondary water-drainage curve
A_2	Area under the imbibition curve falling bellow the zero-P_c axis
$A_{Heptane}$	Reference area between the thiocyanate and sulfate curves generated by flooding a core assumed to be strongly water-wet (saturated with heptane)
A_{Wett}	Area between the thiocyanate and the sulfate curves generated by flooding a core aged in crude oil.
C	Concentration of effluent ions, mole/l
C_0	Concentration of injected ions, mole/l
C/ C_0	Relative concentration of effluent ions
EOR	Enhanced oil recovery
g	Acceleration due to gravity, m/s^2
g_c	Conversion factor

H	Height of liquid column, m
IAH	Amott-Harvey index
IFT	Interfacial tension, mN/m
I_o	Amott oil index
IOIP	Initial oil in place
IOR	Improved Oil recovery
I_w	Amott water index
k	Absolute permeability. m^2 or mD
k_c	Relative permeability of non-wetting phase
k_w	Relative permeability of water
L	Capillary-tube length, m
L	Core length, cm
m	Core weight wet, g
m_0	Core weight dry, g
N_w	Wettability number, USBM
OHIP	Original hydrocarbons in place
p_1	Pressure in a fluid, Pa
p_2	Pressure in a fluid, Pa
P_c	Capillary pressure, Pa
PV	Pore volume, cm^3
r	Radius
R_1	Largest principal radii of a curvature
R_2	Smallest principal radii of a curvature
S_{or}	Residual oil saturation, fraction or %
SSW	Synthetic seawater
SW-U	Modification of SSW, without sulfate and thiocyanate
SW-½M	Modified seawater with half the sulfate concentration and thiocyanate as tracer
SW-¼M	Modified seawater with forth the sulfate concentration
S_w	Water saturation, fraction or %
S_{wc}	Saturation of wetting phase, fraction or %
S_{nc}	Saturation of non-wetting phase, fraction or %
S_{wi}	Initial water saturation, fraction or %
S_{wi}	Initial water saturation, fraction or %

V_p	Pore volume, cm^3
V_b	Bulk volume, cm^3
V	Volume cm^3
$\overline{v}$	Average velocity in capillary tube, m/s
WI_{New}	New wettability index
W_{wet}	Core weight wet, g
W_{dry}	Core weight dry, g

9 References

Al-Hadhrami, Hamed S., Petroleum Development Oman, and Blunt, Martin J., Imperial College. 2001. Thermally Induced Wettability Alteration to Improve Oil Recovery in Fractured Reservoirs. Paper SPE 71866 revised for publication from paper SPE 59289 presented at the 2000 SPE/DOE Improved Oil Recovery Symposium, Tulsa, Oklahoma, 3-5 April

Andersen, Mark A. Petroleum Research in North Sea Chalk. 1995. Amoco Norway Oil Company and RF-Rogaland Research. ISBN 82-7220-725-7

Anderson, William G., Conoco Inc. 1986. Wettability Literature Survey – Part 1: Rock/Oil/Brine Interactions and the Effect of Core Handling on Wettability. Paper SPE 13932. Journal of Petroleum Technology, October 1986

Austad, T and Milter, J. RF Rogaland Research. 1997. Spontaneous Imbibition of Water Into Low Permeable Chalk at Different Wettabilities Using Surfactants. Paper SPE 37236 was presented at the International Symposium on Oilfield Chemistry held in Houston, TX, 18-21 February 1997

Austad, T., Strand, S., Høgnesen, E.J., and Zhang, P., Stavanger U. College 2005. Seawater as IOR Fluid in Fractured Chalk. Paper SPE 93000 was presented at the 2005 SPE International Symposium on Oilfield Chemistry held in Houston, Texas, U.S.A. 2-4 February 2005

Cole, Frank W. Reservoir Engineering Manual. 1969. Golf Publishing Company, Houston, Texas. Printed in U.S.A. Library of Congress Catalog Card Number 60-16853

Cossé, R. Basics of reservoir engineering. Oil and gas field development techniques. 1993. Éditions Technip, Paris. ISBN 2-7108-0630-4. Printed in France by Imprimerie Nouvelle, 45800 Saint-Jean-de-Braye

Dake, P.L. Fundamentals of Reservoir Engineering. Developments in petroleum science 8. 1978. Elsevier Scientific Publishing Company. Printed in The Nederlands. ISBN 0-444-41830-X

Dake, P.L. The practice of Reservoir Engineering. Developments in petroleum science 36. 1994. Elsevier Scientific Publishing Company. Printed in The Nederlands. ISBN 0-444-88538-2

Gluyas, Jon and Swarbick, Richard Petroleum Geoscience. 2004. Blackwell Science Ltd a Blackwell Publishing company. Printed in U.K. ISBN 0-632-03767-9

Green, Don W. and Willhite, G. Paul. Enhanced Oil Recovery. SPE textbook series vol.6. 1998 Henry L. Doherty Memorial Fund of AIME Society of Petroleum Engineers Richardson, TX USA. ISBN 978-1-55563-077-5

Hirasaki, George and Zhang, Danhua Leslie, Rice University. 2003. Surface Chemistry of Oil Recovery From Fractured, Oil-Wet, Carbonate Formation. Paper SPE 80988 presented at the SPE International Symposium on Oilfield Chemistry held in Houston, Texas, U.S.A., 5-8 February 2003

Høgnesen, E.J., Strand, S. and Austad, T. U. of Stavanger 2005. Water flooding of Preferential Oil-Wet Carbonates: Oil recovery Related to Reservoir Temperature and Brine Composition. Paper SPE 94166 presented at the SPE Europrec/EAGE Annual Conference held in Madrid, Spain, 13-16 June 2005.

Korsnes, R.I., Strand, S., Hoff, Ø., Pedersen, T., Madland, M.V., Austad, T. Eurock 2006, Does the chemical interaction between seawater and chalk affect the mechanical properties of chalk? Multiphysics Coupling and Long Term Behavior in Rock Mechanics- Cottheim, A.V., Charlier, R., Thimus, J.F. and Tshibangu, J.P. (eds), Taylor & Francis, London, (2006), pp. 427-434. ISBN 0 415 41001 0

Manrique, E.J. Norwest Questa Engineering; Muci, V.E., Florida Intl. U.; and Gurfinkel, M.E., U. of Texas at Austin. 2006. EOR Field Experiments in Carbonate Reservoirs in the United States. Paper SPE 100063 was presented at the 2006 SPE/DOE Symposium on Improved Oil Recovery held in Tulsa, Oklahoma, U.S.A., 22-25 April 2006

Morrow, Norman R.. New Mexico Petroleum Recovery Research Center, New Mexico Inst. of Mining & Technology. 1990. Wettability and Its Effect on Oil Recovery. Paper SPE 21621. Society of Petroleum Engineers, December 1990

Namba, T. and Hiraoka, T., Zakum Development Company. 1995. Capillary Force Barriers in a Carbonate Reservoir Under Water flooding. Paper SPE 29773 was presented at the SPE Middle East Oil Show held in Bahrain, 11-14 March 1995.

Selly, Richard C. Elements of Petroleum Geology. 1998. Second edition. Printed by Academic Press, U.S.A. ISBN 0-12-636370-6

Siagi, Z.O., Mbarawa, M., Mohamed, A.R., Lee, K.T., Dahlan, I.. Department of Mechanical Engineering, Tshwane University of Technology Pretoria, South Africa, School of Chemical Engineering, University Sains Malaysia, Seri Ampangan, Pulau Pinang, Malaysia. 2007. The effects of limestone type on the sulphur capture of slaked lime. Fuel 2007.

Skjæveland, Svein M. and Kleppe, Jon. SPOR MONOGRAPH. Recent Advances in Improved Oil Recovery Methods for North Sea Sandstone Reservoirs. Norwegian Petroleum Directorate, Stavanger, 1992. ISBN 82-7257-340-7 YA 753

Strand, Skule, Høgenesen, Eli J., Austad, Tor. Stavanger University, Department of Petroleum Engineering. 2005. Wettability alteration of carbonates – Effects of potential determining ions (Ca^{2+} and SO_4^{2-}) and temperature. Colloids and Surfactants A: Physicochem. Eng. Aspects 275 (2006) 1-10

Strand, S., Standnes, D.C., Austad, T. 2006. New wettability test for chalk based on chromatographic separation of SCN^- and SO_4^{2-}. Journal of Petroleum Science and Engineering 52 (2006) 187-197

Treiber, L. E., Archer, Duane L, Owens, W.W. Amoco Production Co. Tulsa Okla. 1972. A Laboratory Evaluation of the Wettability of Fifty Oil-Producing Reservoirs. Paper SPEJ 3526 p.531-540 was presented at SPE 46th Annual Fall Meeting, held in New Orleans, Oct 3-6, 1972

Tweheyo, M.T., Zhang, P. and Austad, T.. U. of Stavanger. 2006. The Effects of Temperature and Potential Determining Ions Present in Seawater on Oil Recovery From Fractured Carbonates. Paper SPE 99438 was presented at the SPE/DOE Symposium on Improved Oil Recovery held in Tulsa, Oklahoma, U.S.A. 22-26 April 2006.

Zhang, P. and Austad, T., U. of Stavanger 2005a. Water flooding in Chalk: Relationship Between Oil Recovery, New Wettability Index, Brine Composition and Cationic Wettability Modifier. Paper SPE 94209 WAS presented at the SPE Europrec/EAGE Annual Conference held in Madrid, Spain, 13-16 June 2005

Zhang, P. and Austad, T., Stavanger U. College. 2005b. The Relative Effects of Acid Number and Temperature on Chalk Wettability. Paper SPE 92999 was presented at the 2005 SPE International Symposium on Oilfield Chemistry held in Houston, Texas, U.S.A. 2-4 February 20005.

Zolotukhin, Anatoly B. and Ursin, Jann-Rune. Introduction to Petroleum Reservoir Engineering. Høyskoleforlaget AS 2000. ISBN 82-7634-065-2

Appendix A

Spontaneous imbibition

Core # SK, 2-3 md, 20°C, imbibition brine SSW

Days	Volume [ml]	Recovery [%]
0,00	0,00	0,00
0,00	0,20	0,72
0,01	0,30	1,08
0,01	0,40	1,44
0,01	0,50	1,80
0,01	0,60	2,16
0,01	0,80	2,87
0,01	1,00	3,59
0,02	1,40	5,03
0,02	1,70	6,11
0,02	2,50	8,98
0,02	2,90	10,42
0,03	4,50	16,17
0,03	5,10	18,32
0,03	6,20	22,28
0,03	7,40	26,59
0,04	8,40	30,18
0,04	10,80	38,80
0,05	12,80	45,99
0,05	14,20	51,02
0,05	15,80	56,77
0,06	16,70	60,00
0,06	17,90	64,31
0,07	18,90	67,90
0,08	19,30	69,34
0,09	19,60	70,42
0,10	19,80	71,14
0,11	20,00	71,86
0,13	20,10	72,22
0,18	20,30	72,93
1,00	21,20	76,17
2,25	21,50	77,25
3,26	21,60	77,61
3,99	21,60	77,61
5,01	21,70	77,96
5,97	21,70	77,96
11,17	21,90	78,68
22,03	22,10	79,40

Core # 20A, 3.03 mD, imbibition brine SSW

Temperature	Days	Volume [ml]	Recovery [%]
20°C	0,00	0,00	0,00
-	0,98	0,10	0,69
-	2,23	0,20	1,38
-	3,24	0,28	1,93
-	3,96	0,38	2,62
50°C	4,01	0,38	2,62
-	4,04	0,60	4,14
-	4,07	0,70	4,83
-	4,16	0,80	5,52
-	4,22	0,90	6,22
-	4,38	0,90	6,22
-	4,98	1,10	7,60
-	5,14	1,20	8,29
-	6,00	1,25	8,63
-	6,95	1,30	8,98
-	8,13	1,40	9,67
-	10,95	1,50	10,36
70°C	12,00	1,50	10,36
-	12,07	1,60	11,05
-	12,13	1,70	11,74
-	12,27	2,00	13,81
-	12,50	2,00	13,81
-	12,95	2,15	14,85
-	13,12	2,20	15,19
-	13,95	2,30	15,88
-	15,10	2,40	16,57
-	17,95	2,50	17,26
-	21,00	2,60	17,96
-	23,96	2,70	18,65
-	28,96	2,75	18,99

Core # 12D, 20.40 mD, imbibition brine SSW

Temperature	Days	Volume [ml]	Recovery [%)
20°C	0,00	0,00	0,00
50°C	3,99	0,00	0,00
-	4,05	0,15	1,03
-	4,10	0,20	1,38
-	4,15	0,40	2,76
-	4,21	0,50	3,45
-	4,37	0,50	3,45
-	4,97	0,50	3,45
-	5,12	0,55	3,79
-	5,99	0,57	3,93
-	6,94	0,58	4,00
-	8,11	0,58	4,00
-	10,94	0,59	4,07
70°C	11,99	0,60	4,14
-	12,06	0,70	4,82
-	12,11	0,80	5,51
-	12,25	0,85	5,86
-	12,49	0,90	6,20
-	13,10	0,95	6,55
-	13,93	1,10	7,58
-	15,09	1,13	7,79
-	17,94	1,23	8,48
-	24,94	1,30	8,96
-	28,95	1,40	9,65

Core # 46A, 2.24 mD, imbibition brine SSW

Temperature	Days	Volume [ml]	Recovery [%]
20°C	0,00	0,00	0,00
50°C	1,97	0,05	0,34
-	2,02	0,40	2,68
-	2,05	0,50	3,35
-	2,09	0,60	4,03
-	2,22	0,62	4,16
-	3,03	0,65	4,36
-	4,94	0,70	4,70
70°C	5,95	0,70	4,70
-	6,00	0,90	6,04
-	6,09	1,00	6,71
-	6,28	1,50	10,06
-	6,95	2,20	14,76
-	7,13	2,90	19,46
-	7,19	3,10	20,80
-	8,35	3,20	21,47
-	9,01	3,35	22,48
-	10,16	3,50	23,48
-	11,96	3,70	24,82
-	13,98	3,90	26,17
-	15,94	3,90	26,17
-	19,98	4,10	27,51

Appendix B

Dionex ion chromatography measurements

Core # 2-21, SW-¼M, diluted 1:10, Q=0.1ml/min, ambient temperature

Sample Name	Thiocyanate [mg/l]	Sulfate [mg/l]	Magnesium [mg/l]	Calcium [mg/l]	Pore Volume
SW0,25M 1:10	70,0000	58,0000	108,0000	52,0000	
SW0,25M 1:50	14,0000	11,6000	21,6000	10,4000	
4	n.a.	n.a.	95,7200	54,0146	0,122
12	n.a.	n.a.	95,8328	54,3078	0,499
13	n.a.	n.a.	96,5336	54,4711	0,541
14	n.a.	n.a.	97,0912	54,6054	0,582
15	n.a.	n.a.	98,5353	55,3041	0,623
16	3,3857	n.a.	98,9678	55,6723	0,667
17	6,7951	n.a.	99,9942	55,3513	0,710
18	14,1088	n.a.	101,4063	54,9683	0,753
20	25,3565	3,4135	105,7328	52,3708	0,837
22	35,6100	8,8959	106,4363	48,8903	0,922
24	40,6304	14,6532	109,2122	48,5458	1,006
26	49,6347	22,3153	112,5481	49,1134	1,093
28	54,4101	29,1691	112,3385	49,1192	1,180
30	57,4604	34,9247	113,9960	50,7776	1,267
32	59,6020	38,9979	115,8660	52,5522	1,350
34	60,0538	41,5682	114,9472	53,4384	1,433
36	66,3827	47,8997	116,0012	54,5469	1,520
38	63,0966	46,7551	115,2791	55,0235	1,607
40	62,4736	47,0259	116,2836	55,9227	1,693
41	63,3077	48,4382	114,5642	55,4878	1,736
42	72,3765	55,7397	115,4898	56,0781	1,779
43	65,7996	51,0997	116,9662	56,7974	1,818
44	73,4941	57,2479	117,0145	56,9015	1,860

Core # 2-21, SW-½M, diluted 1:20, Q=0.1ml/min, ambient temperature

Sample Name	Thiocyanate [mg/l]	Sulfate [mg/l]	Magnesium [mg/l]	Calcium [mg/l]	Pore Volume
SW0,5M 1:20	3,5000	5,7500	5,4000	2,6000	
SW0,5M 1:100	0,6977	1,1513	1,0719	0,5367	
SW0,5M 1:100	0,7023	1,1487	1,0881	0,5033	
2	n.a.	n.a.	4,8374	2,7312	0,033
4,1	n.a.	0,2727	4,8349	2,6914	0,239
4,2	n.a.	0,3028	4,7975	2,7111	0,239
6	n.a.	n.a.	4,8377	2,7118	0,361
8	n.a.	n.a.	4,7759	2,6968	0,446
10	n.a.	n.a.	4,9070	2,7094	0,529
11	n.a.	n.a.	4,8935	2,7066	0,571
12	n.a.	n.a.	4,8718	2,6025	0,613
13	n.a.	n.a.	4,9214	2,7210	0,654
14	n.a.	n.a.	4,9902	2,7495	0,696
15	n.a.	n.a.	4,8771	2,6739	0,739
16	0,4541	n.a.	4,9035	2,6178	0,781
17	0,7701	n.a.	4,9185	2,5467	0,822
18	1,1478	0,3605	4,9682	2,3770	0,866
20	1,9023	1,2023	5,2494	2,1446	0,952
22	2,4756	2,1654	5,4632	2,0400	1,038
24	2,8742	3,1086	5,6027	2,0669	1,123
26	2,9913	3,6785	5,6432	2,1524	1,208
28	3,1598	4,2263	5,7022	2,2723	1,293
30	3,2970	4,6566	5,7596	2,3929	1,377
32	3,3506	4,8654	5,7453	2,4805	1,462
34	3,3336	4,9492	5,6008	2,4790	1,546
36	3,3056	4,9726	5,5975	2,4921	1,629
38	3,2510	4,9400	5,6150	2,5048	1,711
40,1	3,4133	5,2514	5,7132	2,5805	1,793
40,2	3,4839	5,3658	5,6577	2,5957	1,793
41	3,4483	5,3164	5,7527	2,5696	1,835
42	3,7930	5,8569	5,7405	2,5345	1,878
43	3,5362	5,4951	5,6607	2,5480	1,921
44	3,7076	5,7963	5,6823	2,5554	1,964

Core # 20A, SW-½M, diluted 1:20, Q=0.1ml/min, ambient temperature

Sample Name	Thiocyanate [mg/l]	Sulfate [mg/l]	Magnesium [mg/l]	Calcium [mg/l]	Pore Volume
SW0,5M 1:20	3,5000	5,7500	5,4000	2,6000	
SW0,5M 1:100	0,7000	1,1500	1,0800	0,5200	
2	n.a.	0,4630	4,9478	2,5586	-0,004
4	n.a.	n.a.	4,9525	2,5683	0,200
6	n.a.	n.a.	4,9841	2,5769	0,317
8	n.a.	n.a.	4,9468	2,5452	0,399
10	n.a.	0,5305	5,0377	2,5365	0,481
11	0,3556	0,6674	5,0820	2,4906	0,522
12	0,4707	0,8178	5,1497	2,4919	0,563
13	0,6150	1,0058	5,2816	2,4958	0,604
14	0,7820	1,2609	5,3056	2,4742	0,646
15	0,9532	1,4781	5,3619	2,4546	0,687
16	1,1563	1,7756	5,4277	2,4599	0,729
17	1,2972	1,9670	5,4701	2,4518	0,770
18	1,5117	2,3339	5,5295	2,4740	0,811
19	1,6463	2,5041	5,5721	2,4787	0,852
20	1,8280	2,8061	5,5878	2,4857	0,893
22	2,0541	3,1645	5,6227	2,5046	0,974
24	2,2733	3,5018	5,6892	2,5239	1,054
26	2,6856	4,1154	5,7364	2,5310	1,142
28	2,7181	4,2386	5,7487	2,5378	1,223
30	2,8721	4,5584	5,8296	2,5703	1,304
32	2,9992	4,7509	5,8650	2,6089	1,384
34	3,0594	4,8851	5,8393	2,5952	1,467
36	3,1258	5,0016	5,8591	2,6241	1,550
38	3,1972	5,1908	5,9016	2,6433	1,634
40	3,2709	5,2899	5,8922	2,6514	1,716
41	3,3195	5,3474	5,9319	2,6731	1,757
42	3,3177	5,3582	5,8873	2,6553	1,798
43	3,3664	5,4339	5,9255	2,6734	1,839
44	3,3751	5,4663	5,9580	2,6851	1,881

Core # 46A, SW-½M, diluted 1:20, Q=0.1ml/min, ambient temperature

Sample Name	Thiocyanate [mg/l]	Sulfate [mg/l]	Magnesium [mg/l]	Calcium [mg/l]	Pore Volume
SW0,5M 1:20	3,5000	5,7500	5,4000	2,6000	
SW0,5M 1:100	0,7000	1,1500	1,0800	0,5200	
2	n.a.	n.a.	5,0885	2,7540	0,025
4	n.a.	n.a.	4,9965	2,6885	0,225
6	n.a.	n.a.	5,1333	2,7595	0,338
8	n.a.	n.a.	4,9698	2,6849	0,418
10	n.a.	n.a.	5,0041	2,6857	0,498
11	n.a.	n.a.	5,1793	2,7962	0,537
12	n.a.	n.a.	5,1921	2,7994	0,577
13	n.a.	n.a.	5,3034	2,8603	0,617
14	n.a.	n.a.	5,1066	2,7482	0,658
15	n.a.	n.a.	5,8017	3,1498	0,699
16	n.a.	n.a.	5,0726	2,7258	0,739
17	n.a.	n.a.	5,0674	2,7164	0,779
18	0,3434	n.a.	5,4006	2,8568	0,819
19	0,7048	0,1860	5,2324	2,6698	0,859
20	1,1241	0,5528	5,5786	2,7476	0,899
22	1,9057	1,6648	5,3071	2,3665	0,977
24	2,5930	2,9639	5,4215	2,3386	1,056
26	3,0732	4,0528	5,5756	2,3603	1,136
28	3,4025	4,8356	5,5374	2,4020	1,216
30	3,7484	5,5716	5,5568	2,4840	1,295
32	3,6634	5,6040	5,5806	2,6281	1,375
34	4,0959	6,3413	5,6490	2,6338	1,453
36	3,7900	5,9863	5,6213	2,6625	1,532
38	4,3363	6,8531	5,6873	2,6912	1,613
40	4,3078	6,8296	5,5525	2,7232	1,693
41	4,3944	7,0021	5,7732	2,7552	1,733
42	4,1236	6,6399	5,6205	2,7073	1,773
43	4,4902	7,1769	5,6488	2,7090	1,811
44	4,1208	6,6605	5,6371	2,6999	1,850
SW0,5M 1:20 # 2			5,4010	2,6300	
SW0,5M 1:100 # 2			1,0947	0,5321	

Core # 20A, SW-½M, diluted 1:20, Q=0.1ml/min, ambient temperature after the core had been flooded with SSW at 130°C

Sample Name	Thiocyanate [mg/l]	Sulfate [mg/l]	Magnesium [mg/l]	Calcium [mg/l]	Pore Volume
SW-0,5M 1:20 # 1	35,0000	57,5000	54,0000	26,0000	
SW-0,5M 1:100 # 1	7,0000	15,5000	10,8000	5,2000	
2	n.a.	n.a.	52,5342	25,5808	-0,172
4	n.a.	n.a.	53,7498	26,0568	0,032
6	n.a.	n.a.	53,3629	25,8925	0,146
8	n.a.	n.a.	52,9437	25,7810	0,229
10	n.a.	n.a.	53,0324	25,8066	0,312
12	n.a.	n.a.	53,2253	25,9909	0,395
13	n.a.	n.a.	53,4799	26,1709	0,436
14	n.a.	n.a.	53,0321	25,9098	0,478
15	n.a.	n.a.	53,7465	26,2223	0,520
16	n.a.	n.a.	53,7374	26,1087	0,562
17	n.a.	n.a.	54,1254	26,3456	0,604
18	n.a.	n.a.	53,6966	26,1185	0,644
19	n.a.	n.a.	52,5412	25,4189	0,685
20	n.a.	n.a.	52,0243	25,2021	0,726
21	2,5520	n.a.	52,5705	25,1656	0,768
22	4,0275	n.a.	52,0557	24,6674	0,809
24	9,7596	6,8708	52,0867	23,4041	0,892
26	17,3030	11,0495	50,5774	20,0372	0,975
28	23,9663	18,9305	51,9515	17,9470	1,055
30	28,4898	29,2700	53,5088	17,0115	1,136
32	30,7823	37,9451	53,9242	17,7457	1,218
34	32,0369	43,8264	54,1399	19,3153	1,300
36	33,1610	47,8532	53,6730	20,9806	1,384
38	33,3673	49,9716	53,1550	22,2557	1,466
40	34,0699	52,3280	53,5300	23,3240	1,548
41	33,5754	51,9373	53,0263	23,4108	1,589
42	33,8864	53,1306	53,3065	23,8273	1,630
43	34,2772	53,7816	53,6363	24,2156	1,670
44	34,0277	53,7530	53,1837	24,2580	1,711
SW-0,5M 1:20 # 2	35,2797	58,1003	53,0668	25,5801	
SW-0,5M 1:100 # 2	6,8470	15,5336	10,7218	5,1479	

Core # 46A, SSW, Q=1 PV/day, diluted 1:20, 20°C

Sample Name	Sulfate [mg/l]	Magnesium [mg/l]	Calcium [mg/l]	Pore Volume
SSW 1:20 # 1	115,5000	54,0000	26,0000	
SSW 1:100 # 1	23,1000	10,8000	5,2000	
1	110,5301	56,6926	27,3090	-0,223
2	110,9141	56,2844	26,9351	-0,078
3	111,7517	56,9867	27,2981	0,061
4	113,0942	57,5644	27,4038	0,207
5	112,0239	57,7568	27,3882	0,371
6	114,1983	58,9891	27,9220	0,532
7	113,1449	58,4469	27,6307	0,691
8	112,4225	57,7201	27,2859	0,849
10	112,6481	58,0190	27,4421	1,156
12	114,2241	58,3976	27,7778	1,490
14	122,1696	57,1440	27,2793	1,821
16	114,0608	57,6916	27,6261	2,135
18	112,1679	58,0355	27,8562	2,460
20	114,2048	58,3133	27,9810	2,796
22	113,8433	58,5285	28,1265	3,108
24	114,4118	58,8560	28,2241	3,446
26	113,8768	58,5454	28,1105	3,783
28	114,3021	58,8080	28,2275	4,118
30	113,2215	58,2100	27,9336	4,447
32	124,4197	58,7585	28,2003	4,776
34	113,4566	58,4089	28,0693	5,077
36	113,7230	58,5835	28,1014	5,420
38	122,4832	58,3583	28,0639	5,749
40	112,5058	57,9482	27,7897	6,071
SSW 1:20 # 2	118,6346	57,0484	27,4610	
SSW 1:100 # 2	23,5087	11,5175	5,3026	

Core # 46A, SSW, Q=1 PV/day, diluted 1:20, 80°C

Sample Name	Sulfate [mg/l]	Magnesium [mg/l]	Calcium [mg/l]	Pore Volume
SSW 1:20 # 1	115,5000	54,0000	26,0000	
SSW 1:100 # 1	23,1000	10,8000	5,2000	
1	114,3977	48,3930	25,6745	-0,212
2	115,6355	48,8609	26,2427	-0,050
3	116,4404	48,8118	26,3829	0,116
4	116,3888	48,7579	26,3401	0,292
5	115,7248	48,9397	26,4914	0,467
6	115,9175	48,4290	26,2650	0,637
7	117,4084	48,2494	26,1434	0,806
8	116,9548	47,5613	25,7913	0,974
10	117,1296	48,1095	26,4402	1,314
12	116,4544	47,5884	25,9353	1,648
14	116,4892	47,9268	26,1842	1,981
16	115,6158	47,9123	26,2455	2,320
18	116,2124	47,9800	26,2452	2,646
20	114,7970	47,9382	26,3037	2,966
22	115,6636	47,9383	26,0909	3,321
24	116,2436	47,9643	26,1557	3,656
26	113,9211	48,0837	26,1450	3,972
28	116,0458	48,2586	26,2891	4,326
30	115,0907	49,1215	26,8901	4,651
32	115,1095	47,1403	26,1042	4,978
34	115,2404	47,8157	26,1781	5,335
36	116,8561	48,5916	26,5491	5,664
38	115,6438	48,1153	26,4583	5,994
40	116,1542	48,1620	26,3594	6,349
SSW 1:20 # 2	114,3171	48,3947	25,9110	
SSW 1:100 # 2	23,5729	10,5030	4,7677	

Core # 46A, SSW, Q=1 PV/day, diluted 1:20, 100°C

Sample Name	Sulfate [mg/l]	Magnesium [mg/l]	Calcium [mg/l]	Pore Volume
SSW 1:20 # 1	115,5000	54,0000	26,0000	
SSW 1:100 # 1	23,1000	10,8000	5,2000	
1	114,2603	56,7843	27,9728	-0,213
2	117,2795	57,4224	28,3712	-0,048
3	116,2040	57,4304	29,5662	0,124
4	116,6615	57,2038	28,9282	0,301
5	115,6572	57,1848	29,1941	0,458
6	115,4874	57,8374	29,8708	0,603
7	116,0578	57,3965	29,9463	0,764
8	115,6169	57,1896	30,3430	0,927
10	116,2643	57,0125	30,6908	1,261
12	115,7741	56,6485	30,9217	1,605
14	114,7402	56,5289	31,0410	1,932
16	113,8122	57,2284	31,5829	2,281
18	114,4258	56,1317	31,1589	2,620
20	115,3659	57,7038	32,0628	2,942
22	115,8191	57,6564	32,5636	3,287
24	115,3968	57,3095	32,2702	3,628
26	115,5217	57,2957	32,2090	3,949
28	116,0008	57,5313	32,5532	4,298
30	116,7502	56,7835	32,2436	4,626
32	115,3928	56,7762	32,2945	4,954
34	117,4178	57,5650	32,9215	5,312
36	118,7942	57,5119	32,9132	5,631
38	116,0068	57,1490	32,9073	5,984
40	117,4856	57,3365	33,0708	6,295
SSW 1:20 # 2	114,7531	59,2954	28,3335	
SSW 1:100 # 2	24,9915	11,5633	5,6047	

Core # 46A, SSW, Q=1 PV/day, diluted 1:20, 130°C

Sample Name	Sulfate [mg/l]	Magnesium [mg/l]	Calcium [mg/l]	Pore Volume
SSW 1:20 # 1	115,5000	54,0000	26,0000	
SSW 1:100 # 1	23,1000	10,8000	5,2000	
2	128,9129	60,4187	34,3587	-0,031
3	128,8076	59,7578	37,3810	0,131
4	125,8479	58,0721	39,4327	0,292
5	134,1956	60,6554	43,4271	0,458
6	129,2134	58,1373	43,5405	0,634
7	127,4898	56,5048	43,3802	0,810
8	125,4336	53,9731	42,4600	0,975
10	129,6102	55,6171	44,1069	1,297
12	132,5261	58,0531	46,0491	1,640
14	131,6665	56,3392	44,2208	1,981
16	133,2618	57,8626	44,7731	2,306
18	143,9314	57,0124	44,2267	2,654
20	130,8231	56,0117	43,2677	2,990
22	132,5057	56,8404	43,4742	3,319
24	132,3775	56,7756	43,8690	3,676
26	135,9066	57,4691	44,8132	4,027
28	132,1951	57,5765	45,1358	4,373
30	130,1001	57,7042	45,6047	4,706
32	131,2535	55,7948	44,6628	5,025
34	133,7860	56,8142	46,3735	5,377
36	145,6572	55,7651	46,3754	5,710
38	130,4002	55,2814	46,4748	6,039
40	133,4787	54,3551	46,1364	6,325
SSW 1:20 # 2	131,5426	64,1617	31,2382	
SSW 1:100 # 2	26,4640	12,2091	5,9496	